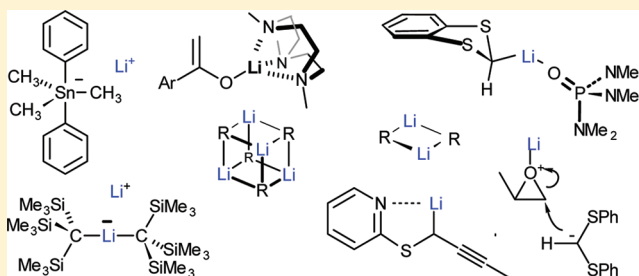


# What's Going on with These Lithium Reagents?

Hans J. Reich\*

Department of Chemistry, University of Wisconsin, Madison, Wisconsin 53706, United States

**ABSTRACT:** This Perspective describes a series of research projects that led the author from an interest in lithium reagents as synthetically valuable building blocks to studies aimed at understanding the science behind the empirical art developed by synthetic chemists trying to impose their will on these reactive species. Understanding lithium reagent behavior is not an easy task; since many are mixtures of aggregates, various solvates are present, and frequently new mixed aggregates are formed during their reactions with electrophiles. All of these species are typically in fast exchange at temperatures above  $-78\text{ }^{\circ}\text{C}$ . Described are multinuclear NMR experiments at very low temperatures aimed at defining solution structures and dynamics and some kinetic studies, both using classic techniques as well as the rapid inject NMR (RINMR) technique, which can in favorable cases operate on multispecies solutions without the masking effect of the Curtin–Hammett principle.



## INTRODUCTION

Organolithium reagents have long played an important role in organic chemistry. The convenient access using cheap, commercially available alkyllithiums and their broad reactivity with almost all functional groups (Figure 1) have resulted in many applications in organic synthesis as well as in the synthesis of many other organometallic compounds, most notably organocopper reagents.

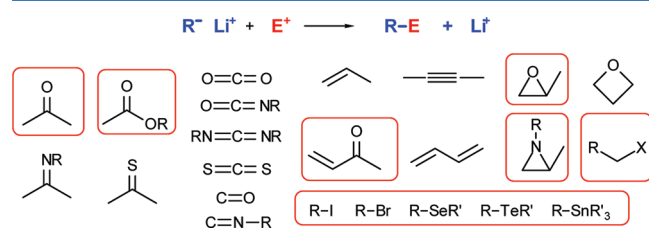
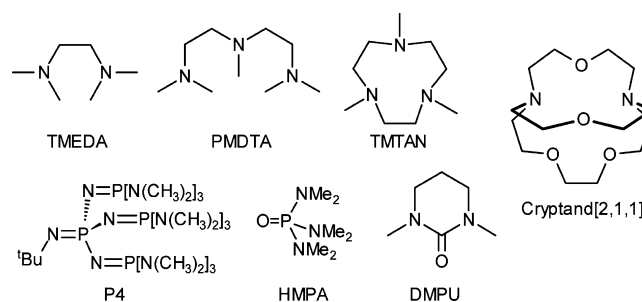


**Figure 1.** Some of the functional groups that react with lithium reagents. This collection does not include the many hundreds of metalations that have been performed. Boxed substrates make an appearance in this Perspective.

In practice, the preparation and utilization of organolithium reagents often involves ad hoc recipes prescribing solvent mixtures, cosolvents, and salt additives. Their complex behavior and importance have encouraged numerous structural and physical organic studies whose early successes include the discovery that most were aggregated in solution and that the degree of aggregation was strongly dependent on carbanion structure, solvent polarity, and the presence of donor ligands like TMEDA, PMDTA, and HMPA. Sometimes the observed aggregates were the actual reactive species; at other times, lower aggregates seemed to be active (from measurement of fractional kinetic orders). These observations raised the interesting and even now only incompletely answered question as to the role

the various aggregates and mixed aggregates play in reactivity and selectivity. Researchers in the area are still mostly in the “gathering anecdotes” phase rather than being in a position to make broad generalizations.<sup>1,2a,3a,4,5a,6</sup> My path into this area started when we were developing organoselenium and organosilicon reagents for use in organic synthesis. At several stages during this work we used heterosubstituted organolithium reagents whose occasionally idiosyncratic behavior had us saying, “Somebody should figure out what’s going on with these lithium reagents.”

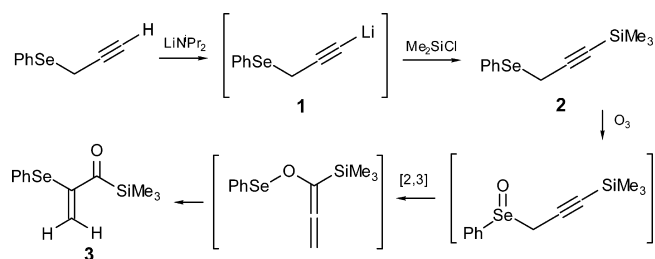


## THE SILYL KETONE CONNECTION

In the late 1970s, we were studying the chemistry of arylseleno organolithium reagents. Among them were  $\alpha$ -lithio selenoxides,<sup>7</sup> lithiated allyl<sup>8a,b</sup> and vinyl selenides,<sup>8b,c</sup> mono- and dilithiated propargyl phenyl selenides,<sup>9</sup> and others.<sup>10–12</sup> Of particular interest in the current context was the simple lithium acetylide **1** which, upon silylation, gave the selenide **2**. Oxidation to selenoxide led, through a series of rearrangements,<sup>9</sup> to the unexpected silyl enone **3**, which introduced us to the chemistry of silyl ketones (acylsilanes).<sup>9b,13</sup>

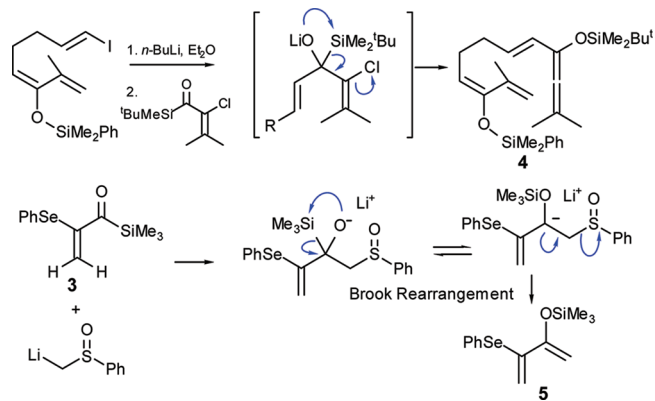
Received: March 9, 2012

Published: May 17, 2012



At this time, Adrian Brook had reported on C to O silyl shifts of  $\alpha$ -silyl alkoxides via  $\alpha$ -siloxy carbanions, a process now known as the Brook rearrangement.<sup>14</sup> We reasoned that complex functionalized  $\alpha$ -silyl alkoxides could be accessed by addition of organometallic reagents to silyl enones such as 3 and, furthermore, that if leaving groups were present at the carbon adjacent to the silicon (the PhSe group could have behaved this way, but did not) elimination could occur to give synthetically valuable enol silyl ethers, previously available only by the silylation of enolates.

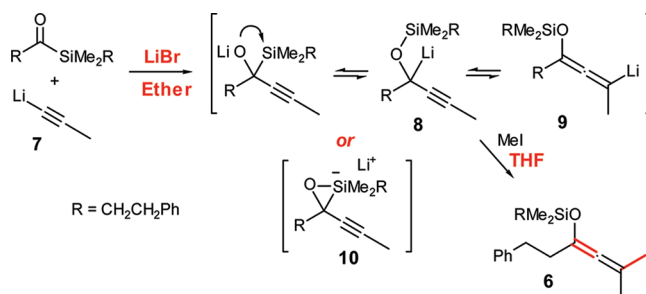
We explored this concept in a series of studies in which the carbanions formed by 1,2-Brook rearrangement were discharged by various elimination reactions. The leaving group could be in the silyl ketone, as in the formation of 4. Alternatively, a leaving group in the lithium reagent provides a method for the acylation of organometallic reagents where the leaving group is not on the acyl group but rather on the organometallic reagent (e.g., formation of 5).<sup>13,15</sup> For each method, in addition to forming a C–C bond, the ketone formed is regioselectively protected/activated as an enol silyl ether, in turn capable of useful chemistry.<sup>16a</sup>



A more advanced use of the Brook carbanion intermediate is reaction with external or internal electrophiles<sup>15a,17</sup> that provides a powerful method in which two C–C bonds can be formed in a single reaction to produce an enol silyl ether.<sup>14b,16b,18</sup> Scheme 1 shows an example in the formation of 6. Similar reactions can be run with vinyl lithium reagents. These processes turned out to be exceptionally sensitive to reaction conditions. The initial acetylide addition must be performed in ether (the reaction failed in THF), and the final alkylation required the addition of THF. This delicate behavior is not surprising considering that one can easily imagine a competition between the original lithium reagent (7) adding to the silyl ketone and the new lithium reagent (8/9) concurrently being formed by Brook rearrangement.

After examples of this method with different silyl ketones, lithium acetylides, and electrophiles had been successfully run, the reaction inexplicably stopped working. This was a vexing

### Scheme 1. Synthetic Application of the Brook Rearrangement<sup>17b</sup>



development, since the process had been publically presented in the interim. After weeks of feverish activity probing every conceivable aspect of the reaction, the student involved (Richard Olson, whose careful record keeping rescued the process) discovered that the batch of lithium diisopropylamide (LDA) used to prepare the lithium acetylide for the successful reactions had been formed with MeLi–LiBr complex. The cheaper *n*-BuLi would have been the normal choice, but a shipment had been delayed. The sudden failures began with a batch of LDA produced using *n*-BuLi. Indeed, when LiBr was added the reaction worked perfectly again, and the student involved and his professor breathed a sigh of relief.<sup>17b</sup> This represents an early example of the profound effects of lithium halides.

This nerve-racking experience provided additional impetus for the initiation of physical organometallic studies to address questions raised during this project and others: the solution structure of lithium acetylides (1, 7), their mechanism of addition to carbonyl compounds, the nature of the potential intermediate allenyl–propargyllithium reagents (8, 9), the origin of the LiBr effect, and the possible intermediate silicon ate complexes (10).<sup>19</sup>

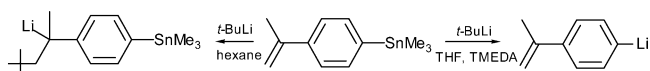
Our entry into the study of organolithium structure and mechanism was also encouraged by the many examples in the literature of striking changes in selectivity and reactivity of organolithium reagents in response to solvent and substrate changes. A few examples are shown in Figure 2.<sup>20a,21–23</sup>

In this Perspective, I outline from a personal point of view some of the research that ensued, roughly in chronological order. Literature citations to my papers are complete, but this is not a review. Citations are sparse to others working in these areas previously, contemporaneously, or subsequent to the work described. I tried to be guided in these efforts by the synthetic origins of our research interest in these species and study lithium reagents that are of more than just mechanistic interest. As shall become clear, we were not immune to the lure of studying “angels dancing on the head of pin” (or HMPA molecules dancing on a lithium) but have attempted to keep in mind the need for utility. The new generation of highly capable multinuclear NMR spectrometers that became available in the early 1980s played a crucial role in addressing these questions.

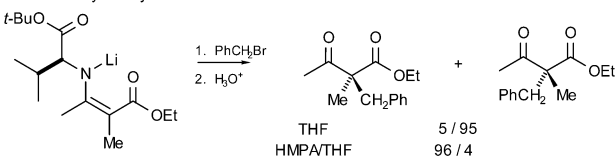
### ■ ALLENYL–PROPARGYLLITHIUMS

Unlike allyllithium reagents, which had been investigated by several research groups,<sup>20b,24a</sup> and intensively studied as synthetic reagents,<sup>25</sup> allenyl–propargyllithium reagents were less well-defined in part because of their propensity for prototropic isomerizations (e.g., to the much more stable alkenyllithiums). The first question we asked was simple: are

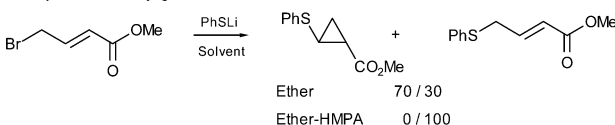
Selectivity between olefin addition and Li/Sn exchange.



Stereochemistry of alkylation



Selectivity between conjugate addition and substitution.



Regioselectivity of Benzene Formation

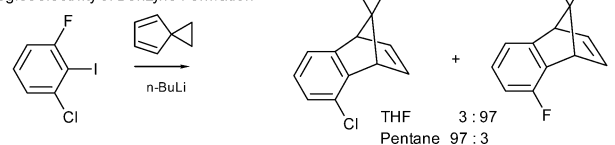
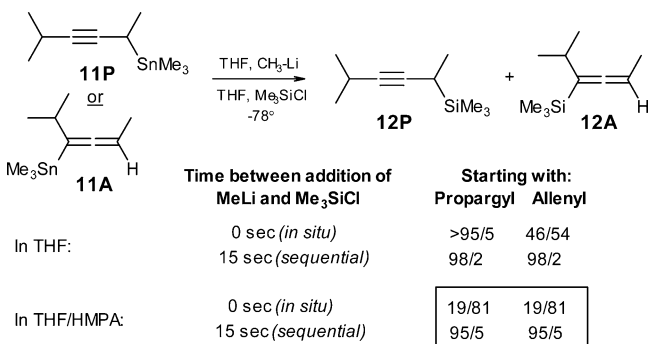


Figure 2. Examples of solvent effects on lithium reagent selectivities.

there two isomeric lithium reagents, and do they have different chemistry? We applied a straightforward test: a pair of isomeric allenyl (A) and propargyl (P) stannanes were converted to lithium reagents by Li/Sn exchange in the presence of suitable electrophiles to see whether different products were formed.

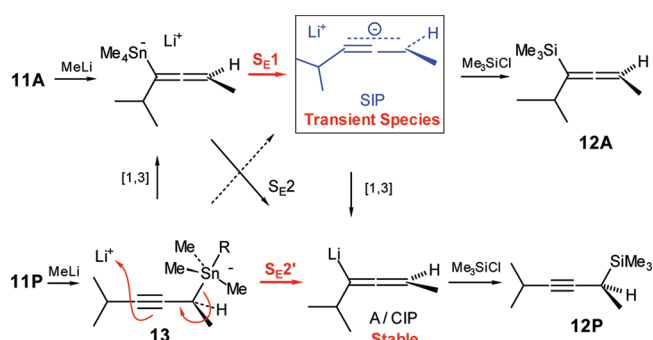
When **11A** or **11P** was converted to lithium reagents by Li/Sn exchange or other methods, such as Li/Se exchange, followed by trimethylsilyl chloride (sequential experiment), both reactions gave the same 98/2 ratio of **12P** to **12A** (Figure 3).<sup>26</sup> However, when the Li/Sn exchanges were performed in

Figure 3. Li/Sn exchange and trapping of allenyl (A) and propargyl (P) stannanes.<sup>26b</sup>

the presence of Me<sub>3</sub>SiCl (in situ experiment) we had a provocative result: **11A** gave slightly more **12A** than **12P** (54/46), and **11P** gave mostly **12P**. We were delighted, but it quickly became clear that there was not a direct connection between the stannane and product isomers. Most decisive was an experiment performed with HMPA present when both **11A** and **11P** gave identical products, which strongly favored the allenyl silane in the in situ experiment and the propargyl silane in the sequential experiment. We concluded there was a transient intermediate which could be trapped by in situ electrophiles to give allenyl silane and a second species, the thermodynamically stable one, which gave propargyl silane.

But what are the two reactive species? The answer to this question came only after extensive solution structure studies of a number of allenyllithium reagents,<sup>27</sup> many Li/Sn exchange experiments on several pairs of A/P isomers with different substituents on the alkyne/allene and the tin, and with different lithium reagents. It also required an excursion into the mechanism of the Li/Sn exchange.<sup>28</sup> Several hypotheses (dimer vs monomer, allenyllithium vs propargyllithium, tin ate complex vs any of several lithium reagent structures, triple ions) were tested. One key observation was that the fraction of *in situ* allenyl product is strongly affected by the substituents on the tin and/or the reagent used for the Li/Sn exchange, suggesting that the Sn ate complex plays an important role. A second was that the in situ generated intermediate is very unselective compared to the sequential one. In a competition between Me<sub>3</sub>SiCl and *i*-PrMe<sub>2</sub>SiCl, the in situ (allenyl product) gives a 58/42 Me/*i*-Pr selectivity, whereas the sequential (propargyl) product gives 98/2.

Eventually we arrived at a mechanistic proposal (Scheme 2) that was consistent with the many features of this process.<sup>26b</sup>

Scheme 2. Mechanism of **11A** and **11P** Conversion to Silanes<sup>26b</sup>

Extensive NMR studies of alkyl-substituted A/P reagents showed that all exclusively possessed the allenyllithium structure and were monomeric in THF (except the parent, which was partially dimeric).<sup>27</sup> We believe the stable species is the allenyllithium (a contact ion pair, CIP), and the transient species is the separated ion pair (SIP). Our studies of the Li/Sn exchange had shown that tin ate complexes are observable intermediates and that in THF solution these are SIPs.<sup>26b</sup> So how do the SIP ate complexes get to be CIP lithium reagents? We can envision the attack of a lithium cation on the stannate in an S<sub>E</sub>2 or S<sub>E</sub>2' process leading directly to the lithium reagents or an S<sub>E</sub>1 process (simple fragmentation of the weak C–Sn bond), which of necessity leads to a highly reactive SIP allenyl anion. This very reactive species rapidly collapses to the stable allenyllithium, but in the presence of an electrophile, it can be captured. The SIP reacts at the allenyl end, since this is the position of highest charge density (Li<sup>+</sup> bonds exclusively to this site).<sup>24c</sup> The stable allenyllithium reacts at the propargyl end (**13**), as is the case for many allenyl organometallic species (the allenyl position is blocked by the lithium). The unusually low steric selectivity of the transient species, the sensitivity to substituents on tin as well as the strong influence of HMPA on the course of the reaction, and other features are all readily explained by this mechanism.

The greater propensity for the propargylstannane to convert to the stable intermediate (the CIP) is reasonable; here, the higher energy propargyl stannate undergoes a favored S<sub>E</sub>2'

process to directly form the stable allenyllithium (as shown for **13**), whereas an  $S_E2'$  process on the allenyl stannate would convert to the higher energy propargyllithium. The effect of HMPA to equalize the reactions starting with **11A** and **11P** and produce more transient species can also be understood (Figure 3); the  $Li^+$  complexed to HMPA is much less electrophilic, suppressing the  $S_E2$  reactions, and favoring  $S_E1$  over  $S_E2$ . The longer lifetime would also give time for the two stannates to equilibrate and afford identical products.

**Solution Structure of Allenyl–Propargyllithium Reagents.** In the course of these studies, we examined the NMR spectra of numerous reagents and found that all alkyl-substituted ones, and those with anion-stabilizing groups at the allenyl carbon ( $C_A$ ), were entirely in the allenyl form (Figure 4). All showed strong C–Li  $J$  coupling at  $C_A$ , none

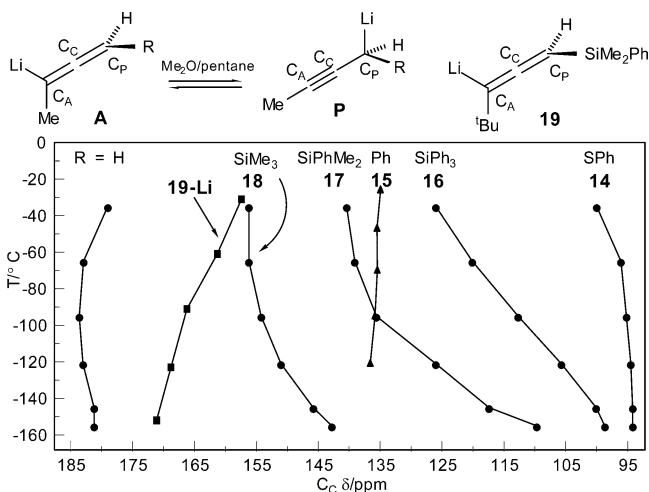
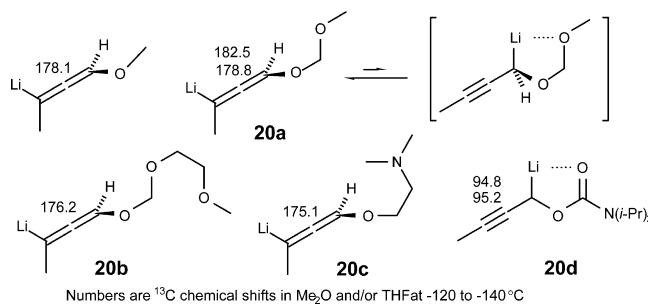


**Figure 4.** Temperature dependence of the  $^{13}C$  NMR chemical shifts of  $C_c$  of some allenyl–propargyllithium reagents in  $Me_2O$ .<sup>27d</sup>

detectable at  $C_p$ .<sup>27b</sup> However, compounds with good carbanion-stabilizing groups at  $C_p$  such as PhS (**14**) and Ph (**15**) are largely in the propargyl form. Compounds with  $R_3Si$  substituents (**16**–**19**) are more variable.<sup>27c,d</sup> The  $^{13}C$  chemical shifts of the central carbon ( $C_p$ ) are especially diagnostic, with estimated values of 100 ppm for the P isomer and 180 ppm for the A isomer. The structures and changes in structure of the  $R_3Si$  compounds (Figure 2) as well as the highly variable Saunders isotope perturbation shifts (comparison of H and D at  $C_p$ )<sup>27e</sup> can be rationalized by closely matched equilibria of the two localized structures and bridged ones ( $\pi$ -complex). The localized structures require a higher degree of solvation than bridged ones. The degree of solvation is a very sensitive function of steric effects at the P and A sites of the carbanion, the size and basicity of the solvent, and, of course, the temperature (less solvation at higher temperature). For example the phenyl-substituted compound **15** in  $Me_2O$  solution shows a very small temperature dependence, gives no detectable Saunders' isotope shift and thus is delocalized (bridged). In THF– $Et_2O$  solution it is a mixture of localized A and P structures.<sup>27e</sup>

We attempted to manipulate the A/P lithium reagent equilibria through chelation effects. In reagents with potentially chelating alkoxy (**20a**, **20b**) and amine (**20c**) substituents at  $C_p$  only the propargyl structure can benefit from chelation. All three were in the unchelated allenyllithium form. However, the more strongly chelating carbamoyl group (in compound **20d**)

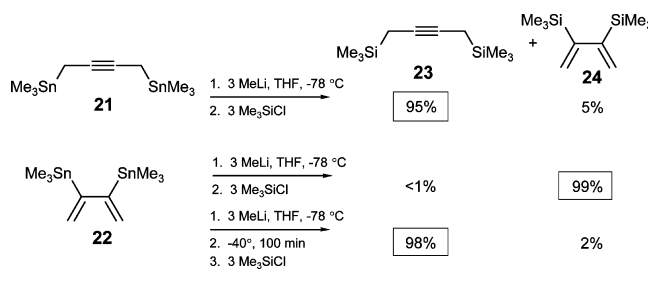
did form entirely the propargyl isomer, although the more electron-withdrawing nature of the substituent could also contribute.<sup>27b,29</sup> The unexpectedly weak chelating effects of ether and amine groups seen here and in other systems prompted several studies in other classes of lithium reagents, as detailed in sections below.<sup>30</sup>



## LITHIUM REAGENTS FROM STANNYLBUTADIENES

In connection with a synthesis of some polychlorinated butadiene metabolites,<sup>31</sup> we were interested in 2,3-hetero-disubstituted butadienes for use in Diels–Alder reactions.<sup>27a,32</sup> In the course of this work, we encountered another system involving allenyl–propargyl anions whose reactions had a puzzling dependence on order of addition and sample history. Treatment of either 2,3-dichlorobutadiene or 1,4-dichlorobutene with  $Me_3SnLi$  gave 1,4-bis(trimethylstannyl)-2-butyne (**21**) under kinetic control and pure 2,3-bis(trimethylstannyl)-butadiene (**22**) under thermodynamic control.<sup>32</sup> When these stannanes were individually subjected to Li/Sn exchange using  $Me_3SiCl$  as electrophile, rather complicated behavior resulted, with the limiting conditions allowing preparation of either isomer of the silylated products from **22** (Scheme 3). The propargyl stannane gave **23** under all conditions.

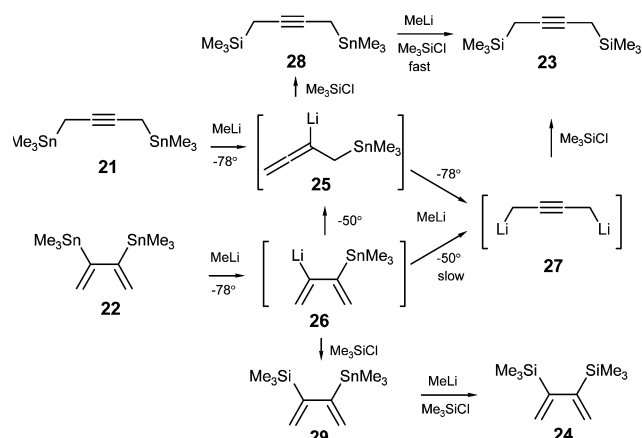
### Scheme 3. Silylation Products of Lithium Reagents Prepared from **21** and **22**<sup>27a</sup>



Examination of the NMR spectra of solutions under various metalation conditions confirmed the structures of **25**, **26**, and **27** (Scheme 4). At  $-78^\circ C$ , stannane **22** undergoes only mono Li/Sn exchange to form **26**, which is silylated to form **29**. A second in situ Li/Sn exchange and silylation forms **24**. At  $-50^\circ C$ , **26** undergoes a second Li/Sn exchange to form **27**, which gives propargyl products only. Stannane **21**, on the other hand, undergoes rapid mono- (to form **25**) and dimetalation (to form **27**), both of which lead to **23**.<sup>27a</sup>

## "ATE" COMPLEX INTERMEDIATES IN THE LITHIUM METALLOID EXCHANGE

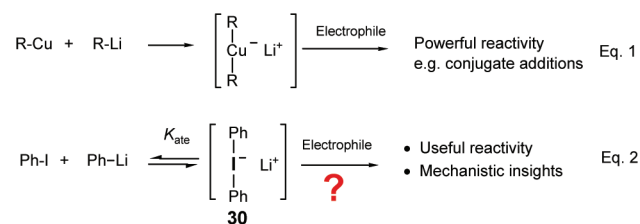
George Wittig was the first to suggest that metal–halogen exchange reactions, one of the premier methods for the

Scheme 4. Pathways from Stannanes 21 and 22 to the Silanes 23 and 24<sup>a</sup>

<sup>a</sup>Intermediates 25–27 were spectroscopically characterized.<sup>27a</sup>

formation of several types of organolithium reagents, might proceed through ate complex intermediates rather than through direct substitutions or other mechanisms, including four-center and SET (single-electron transfer) pathways.<sup>33</sup> Prompted by the remarkable chemistry of organocuprates actively developing in the early 1970s, we asked whether iodine, bromine, or other elements (tin, tellurium, silicon, selenium) formed ate complexes and, if so, whether they might have interesting chemistry in their own right. It is conceivable that some of the reactions attributed to lithium reagents might even be due to ate complexes in equilibrium with them.

We carried out some simple experiments comparing solutions of PhLi alone with those of a solution containing both PhLi and PhI (as well as other species such as PhBr, Ph<sub>2</sub>S, Ph<sub>2</sub>Se, Ph<sub>2</sub>Te, PhSnBu<sub>3</sub>, Ph<sub>3</sub>Bi, Ph<sub>2</sub>Hg).<sup>34a,35a</sup> No significant change in selectivity in 1,2- vs 1,4-additions to enones, Felkin–Anh selectivity with chiral aldehydes, or competitive silylations with different silyl chlorides could be attributed to intervention by species such as Ph<sub>2</sub>I<sup>-</sup> Li<sup>+</sup> (30). However, clear kinetic evidence for such species was found, especially after it was recognized that the equilibrium of eq 2 was strongly



temperature and solvent dependent. THF and especially HMPA moved the equilibrium ( $K_{\text{ate}}$ ) to the right compared to weaker coordinating solvents such as diethyl ether, a consequence of much stronger solvation of Li<sup>+</sup> compared to PhLi. For example, the reactivity of PhLi toward alkylating agents was reduced by a factor of only 2 when excess PhI was added in THF at -78 °C but by at least a factor of 10<sup>6</sup> in THF–HMPA. Such experiments showed that  $K_{\text{ate}}$  became large (>10<sup>7</sup>) and that the reactivity of the ate complex Ph<sub>2</sub>I<sup>-</sup> Li<sup>+</sup> was very much lower than that of PhLi.<sup>34a</sup>

Multinuclear NMR studies of such solutions confirmed that the fourth-row main-group elements I (30),<sup>34a–f</sup> Te (31),<sup>34a,c,f,35a,b</sup> Sn,<sup>28a–c</sup> and Sb<sup>36a</sup> formed easily detectable ate

complexes in the more polar ethereal solvents (Figure 5). In a highly preorganized structure, the third-row element Se formed

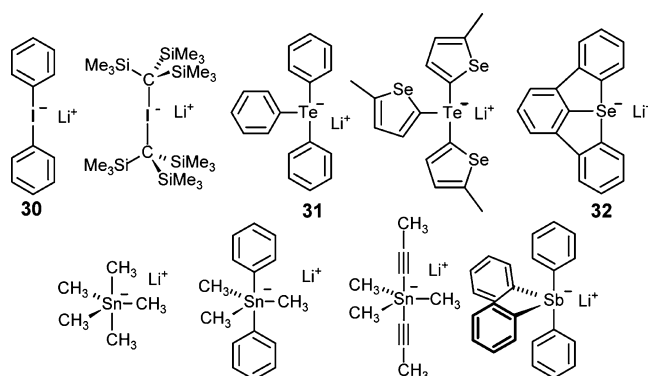


Figure 5. Some of the spectroscopically characterized ate complexes.

such species (32).<sup>35a,c</sup> With suitable substituents, even silicon ate complexes are stable.<sup>37</sup> Ate complexes of these elements with electronegative substituents (O, Cl, F) have long been known; it is the all-carbon substituted compounds that are of interest here.

Full kinetic analysis of the exchange processes of PhLi/PhI and PhLi/Ph<sub>2</sub>Te was complicated by their extreme rate and the presence of two interdependent equilibria (the ate complex equilibrium of eq 2 and the monomer–dimer equilibrium of PhLi). For example, the exchange of eq 2 was rapid on the NMR time scale even at temperatures below -100 °C (Figure 6). A solution of PhLi/PhI in THF at -78 °C undergoes in

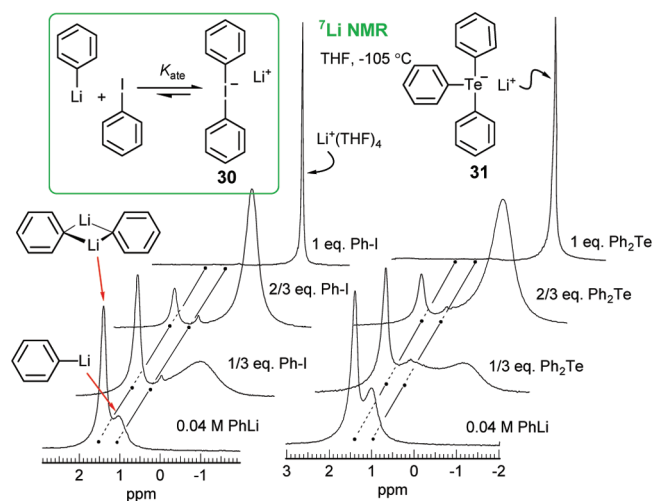


Figure 6. <sup>7</sup>Li NMR study of the exchange of PhLi with PhI and Ph<sub>2</sub>Te at -105 °C in THF. At this temperature  $K_{\text{ate}}$  is large, and only the ate complexes 30 and 31 (no PhLi) can be detected when a full equivalent of PhI or Ph<sub>2</sub>Te is added.<sup>34c</sup>

excess of 10<sup>4</sup> exchanges per second.<sup>34b,36a</sup> That such solutions are stable over a period of days is perhaps the most convincing evidence that SET mechanisms cannot be operative in even a tiny fraction of the exchanges, since it would require cage effects of unrealistic magnitude to avoid destruction of phenyl radicals. The search for a system that could be fully analyzed involved study of not just phenyl, but also aryllithiums from thiophene, selenophene, and diphenylphosphinythiophene

(the latter two were chosen to take advantage of the NMR properties of  $^{77}\text{Se}$  and  $^{31}\text{P}$ ).

The DNMR studies of the lithium iodine exchange showed that only monomeric  $\text{ArLi}$  reagents participated in the process and dimer was not detectably involved, except as a source of monomer. See Figure 6 where the line shape of the dimer  $\text{PhLi}$  signal is unaffected by the presence of  $\text{PhI}$  or  $\text{Ph}_2\text{Te}$  but the monomer is near coalescence with the ate complex lithium. These experiments provided an early estimate of relative aggregate reactivity, with monomer at least 3 orders of magnitude faster than dimer in the  $\text{Li}/\text{I}$  exchange.<sup>34d,36a</sup>

The NMR studies also demonstrated that the iodine ate complexes themselves were involved in the exchange as aryl anion donors and in one experiment were 1/40 as reactive as  $\text{ArLi}$  monomer.<sup>34b,d,36a</sup> It is interesting that in more typical reactions (carbonyl addition, alkylation reactions)  $\text{Ar}_2\text{I}^- \text{Li}^+$  was demonstrably several orders of magnitude less reactive than the  $\text{ArLi}$ .

Figure 7 shows a rate summary of some of the  $\text{Ph}_n\text{M}/\text{Ph}_{n+1}\text{M}^-$  exchanges we have studied, compared with the

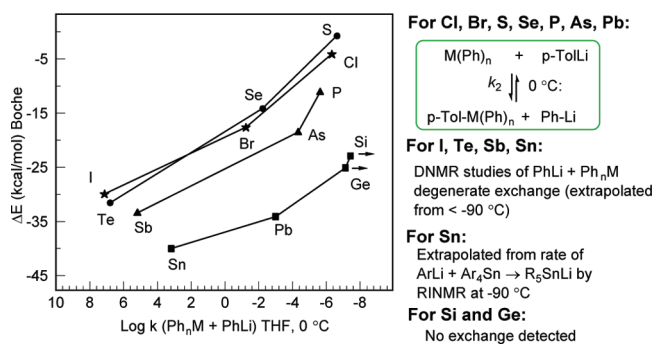


**Figure 7.** Rates of lithium/metalloid exchange reactions, compared with calculated ate complex energies.

computed formation energy of the  $\text{Me}_{n+1}\text{M}^-$  ate complexes.<sup>38</sup> Although the correlation is poor overall, there is a reasonable correlation within a single column of the periodic table, providing some support that all proceed through ate complex intermediates.<sup>39</sup> These data show why the  $\text{Li}/\text{I}$ ,  $\text{Li}/\text{Te}$  and  $\text{Li}/\text{Sn}$  exchanges are the most reliable and least complicated by side reactions since they are over 4 orders of magnitude faster at  $0^\circ\text{C}$  than the next fastest, the  $\text{Li}/\text{Br}$  exchange.<sup>35a,36a</sup> At the temperatures where these reactions are normally done ( $-78^\circ\text{C}$ ), the difference is much larger.

**Stereochemical Course of the  $\text{Li}/\text{Sn}$  Exchange.** While trying to understand the role of ate complexes in the  $\text{Li}/\text{Sn}$  exchange we addressed the question of the stereochemistry *at tin* of this exchange. The stereochemical course at carbon is invariably retention.<sup>28c</sup> We determined the stereochemistry at a nonstereogenic tin center by using substitution by an isotopically labeled nucleophile, taking advantage of a diastereotopic chemical effect (Figure 8). The process works as follows: consider the stannane **33**, in which one of the  $\text{Sn}-\text{CH}_3$  groups (the *exo*) is substituted substantially more rapidly than the other. In a retention process the *exo*  $\text{CH}_3$  group will be replaced by  $\text{CD}_3$  at the rate of the fast process, but the *endo* much more slowly, since only the slow *endo* attack can replace that methyl group (if  $k_{\text{slow}} = 0$ , the *endo* can never be replaced). In an inversion or random process, both methyl groups will be replaced at the fast rate. Experimentally, the rate difference was a factor of 12.5 in ether, large enough that the retention and

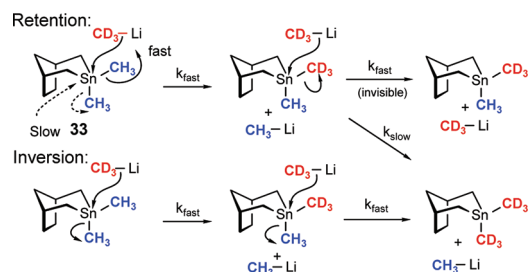
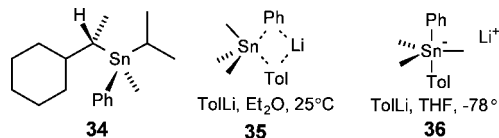


**Figure 8.** Determination of stereochemical course of the  $\text{Li}/\text{Sn}$  exchange at a nonstereogenic center in **33**.<sup>28c</sup>

inversion processes gave very distinct exchange profiles. The substitution occurred with exclusive retention of configuration.

In other experiments on diastereomerically enriched **34** we were able to show that substitution of  $\text{Ph}$  by  $\text{Tol-Li}$  proceeded with at least 99.7% retention in ether, as expected for a four-center mechanism illustrated by **35**, whereas in  $\text{THF}$  the process gave complete equilibration via the freely pseudorotating stannate **36**. The greater influence of lithium cation contacts with the anion in determining the course of reactions when less strongly coordinating solvents are used is a general phenomenon in organolithium mechanisms. For example, a four-center interaction related to that shown in **35** is responsible for the strong preference for 1,2-addition of some lithium reagents to enones in ether, whereas 1,4-addition is seen in  $\text{THF}$  (see below).<sup>40</sup>



## HMPA COMPLEXES OF LITHIUM SPECIES

The strongly coordinating cosolvent HMPA played an important role in understanding the spectroscopy and chemistry of ate complexes through its profound effects on ate complex equilibria, allowing the preparation of solutions of pure ate complexes which had only weak association constants in  $\text{THF}$ . For example, solutions of  $\text{Me}_4\text{Sn}$  and  $\text{MeLi}$  did not form detectable amounts of  $\text{Me}_5\text{Sn}^- \text{Li}^+$  in  $\text{THF}$ , but with 3 equiv of HMPA quantitative formation was observed.<sup>28a</sup> In the course of the NMR studies related to these experiments, we found that below  $-120^\circ\text{C}$   $J$  coupling was observed between  $\text{P}$  and  $\text{Li}$  ( $^2J_{\text{LiP}}$ ) in the  $^7\text{Li}$ ,  $^6\text{Li}$ , and  $^{31}\text{P}$  NMR spectra. The first to be detected was the 1:4:6:4:1 quintet of lithium bonded to four HMPA molecules ( $\text{Li}(\text{HMPA})_4^+$ ), the counterion to the iodine ate complex **30**.<sup>34b</sup> The observation of this easily recognized signal *proves* that the lithium is no longer bonded to the anion (i.e., a SIP has formed). This simple method of assessing lithium ion coordination had important implications and we developed it into a technique for gaining unprecedented insight into ion pair status (SIP/CIP), aggregation state (monomers, dimers, trimers, etc.) and solvation.<sup>41</sup> Figure 9 shows a typical HMPA titration of a SIP (**37**) and a monomeric CIP species (**38**).

The generalizations below were gleaned from HMPA titrations of over 120 lithium species which we have performed over the last 20 years.<sup>18,27d,30c,e,40,41b-d,42,43a,b</sup> Several other laboratories have also reported such experiments.<sup>2b,44-46</sup> In the discussion below, the “R<sup>-</sup>” species can be either a carbanion or

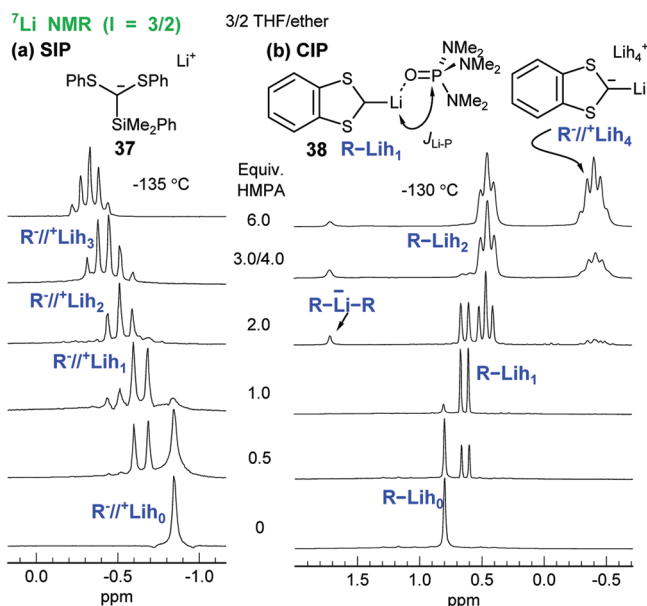


**Figure 9.** HMPA titrations of a SIP and CIP followed by  $^7\text{Li}$  NMR spectroscopy ( $h = \text{O}=\text{P}(\text{NMe}_2)_3$ ). (a) Characteristic pattern of an SIP lithium species (37) in which the lithium cation is sequentially solvated by one to four HMPA molecules, leading to a doublet, triplet, quartet, and quintet in the  $^7\text{Li}$  NMR spectrum from two-bond coupling to the spin 2  $^{31}\text{P}$  nuclei. Free HMPA appears at 4 equiv. (b) Monomeric CIP 38 first coordinates to one and then two HMPA molecules before ion-pair separation occurs to form  $R//\text{Li}(\text{HMPA})_4^+$ . The  $^{31}\text{P}$  NMR spectra show free HMPA when 2 equiv is present.

any other anion. Halides, alkoxides, enolates, thiolates, selenolates, phosphides, and stannides are some that have been examined.

**Separated Ion Pairs.** There are several criteria by which a SIP  $R//\text{Li}^+$  in an HMPA titration can be recognized, but the most important one is that *solvation by HMPA ( $h$ ) proceeds sequentially through the four solvates  $\text{Li}h_n^+$ ,  $n = 1-4$ , in a characteristic pattern, more or less independent of the counterion  $R^-$ , in which the stoichiometric solvate is always the dominant one* (Figure 9a). These species can each be recognized by the multiplicity of the  $^7\text{Li}$  signals due to coupling with  $n$   $^{31}\text{P}$  nuclei. Free HMPA appears only after 3 equiv of HMPA have been added (the HMPA affinity of free lithium cation is high).

**Monomeric CIP Lithium Reagents.** In contrast, a monomeric CIP with a reasonably strong R-Li association does not follow such a sequence. First, the lithium chemical shifts will often be significantly downfield ( $>0.5$  ppm) from those of the SIP species. Second, free HMPA often appears earlier in the titration of a CIP than of a SIP. Most importantly, *if the R-Li species undergoes ion-pair separation, it often largely or entirely "skips" a solvation structure, going, for example, from CIP  $R-Li_1$  to SIP  $R//\text{Li}h_3^+$  (sometimes even skipping two solvates)*. Thus, the stoichiometric solvate  $\text{Li}(\text{HMPA})_2^+$  may be largely absent at 2 equiv of HMPA. In the example in Figure 9b, the titration of 38 proceeds from CIP  $R-Li_2$  to SIP  $R//\text{Li}h_4^+$ ; no  $\text{Li}h_3$  species was detected. This compound, like a number of others,<sup>34e,47</sup> forms significant fractions of triple ions of the  $R_2\text{Li}^- \text{Li}^+$  type.

**Dimeric Lithium Reagents.** When RLi dimers are present,<sup>30c,41b,43a</sup> the HMPA titrations take a more complicated course in which mono- and bis-HMPA-solvated dimers can be

detected, followed by one or more monomeric CIP species. Sometimes ion-pair separation occurs.

**Tetrameric Lithium Reagents.** The few that have been studied ( $\text{MeLi}$ ,<sup>41b</sup>  $\text{ArOLi}$ ,<sup>43a,46</sup>  $\text{Li-enolates}$ <sup>43a</sup>) typically go through a series of HMPA-complexed tetramers, with lower aggregates rarely appearing late in the titration. SIPs are not seen. Free HMPA appears even before 1 equiv of HMPA has been added (i.e., the HMPA affinity of the triply coordinated lithiums is low).

Figure 10 summarizes some information about the ease of ion pair separation for a number of RLi species. Several trends

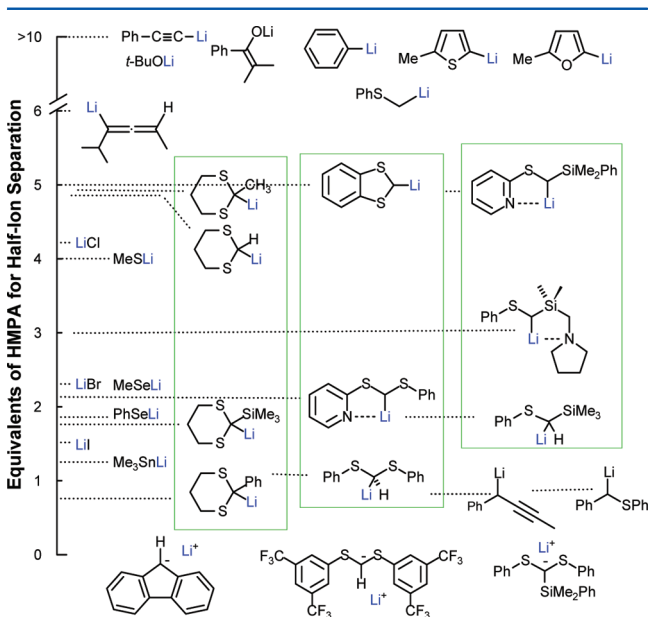


**Figure 10.** Relative ease of ion-pair separation for some lithium reagents in THF or 3:2 THF/ether at  $-120$  to  $-140^\circ\text{C}$  as measured by the equivalents of HMPA needed for half-ion separation (1:1 CIP/SIP). The RLi species at the top do not undergo detectable ion separation with HMPA, the ones at the bottom are SIP in THF. Anion stabilizing substituents generally result in easier SIP formation. Chelating substituents inhibit it (illustrated by the boxed compounds).

are seen: Localized charge makes ion separation difficult, delocalizing substituents make it easier. For lithium bonded to heteroatoms the size of the anion is a better predictor than  $\text{p}K_a$  of the conjugate acid (compare  $\text{LiI}$  and  $\text{SnMe}_3\text{Li}$ ). Chelating groups tend to favor CIPs more than nonchelated analogs. These effects have strong chemical consequences since SIP species can have dramatically different chemistry and reactivity than CIP species.

**HMPA-Bridged Dimers.** In the course of these investigations, we encountered two unusual HMPA solvated dimers. HMPA titrations in diethyl ether (but not in THF) sometimes formed triple-HMPA-bridged dimers. This structural type was best characterized for  $\text{Bu}_3\text{SnLi}$ . At 1 equiv of HMPA, the normal monomeric HMPA complex is formed (Figure 11a). At 1.5 equiv a new species dominates, where the  $^{119}\text{Sn}$  was coupled to a single  $^7\text{Li}$ , each  $^{31}\text{P}$  was coupled to two  $^7\text{Li}$  nuclei, and the  $^7\text{Li}$  to one  $^{119}\text{Sn}$  and three  $^{31}\text{P}$  nuclei. This uniquely defines the structure 39 shown (Figure 11b).<sup>41c</sup> Remarkably, the addition of HMPA causes a monomeric species to form a dimer. Such HMPA-bridged dimers were also detected for  $\text{PhLi}$  and for  $\text{LiBr}$ .<sup>48</sup>

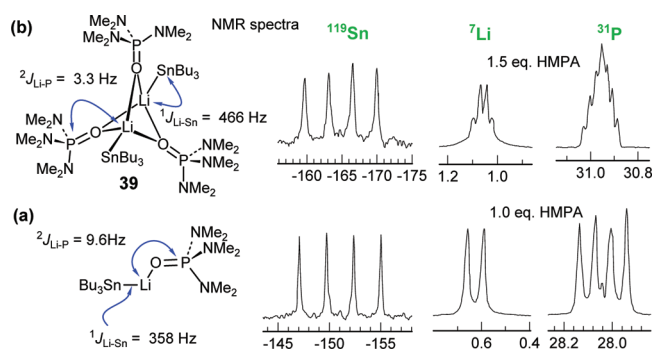
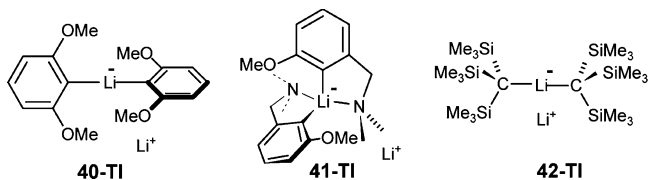


**Figure 11.** Interaction of  $\text{Bu}_3\text{SnLi}$  with HMPA in diethyl ether at  $-120^\circ\text{C}$ . (a) Mono complex, with  $^{119}\text{Sn}$  and  $^{31}\text{P}$  each showing a 1:1:1:1 quartet from coupling to one  $^7\text{Li}$  ( $I = 3/2$ ). The doublet in the  $^7\text{Li}$  NMR is from coupling to  $^{31}\text{P}$ .  $^{119}\text{Sn}$  satellites can be seen in the  $^7\text{Li}$  NMR spectrum. (b) Formation of  $(\text{Bu}_3\text{SnLi})_2(\text{HMPA})_3$  **39** at 1.5 equiv of HMPA. The 1:1:1:1 quartet in the  $^{119}\text{Sn}$  spectrum arises from  $J$  coupling to one  $^7\text{Li}$  nucleus, the 1:2:3:4:3:2:1 septet in the  $^{31}\text{P}$  spectrum from coupling to two  $^7\text{Li}$ . Addition of more HMPA results in formation of the SIP.<sup>47c</sup>

**Triple Ions.** In THF–HMPA solutions, triple ions of the  $\text{R}^-\text{Li}^+\text{R}^-$  type were identified frequently as a significant or even major constituent (e.g., **40** and **41**). Their signature in  $^7\text{Li}$  NMR spectra was a central lithium signal (often broad due to unusually fast quadrupolar relaxation) well downfield of monomer signals (typically  $\delta$  1.5–5) and the early appearance of a  $\text{Li}(\text{HMPA})_4^+$  quintet during an HMPA titration.<sup>47</sup> Almost all aryllithium reagents<sup>30c,d,42</sup> showed partial conversion to triple ions. Some, like 2,6-dimethoxyphenyllithium, formed more than 50% of the triple ion **40-TI** when 2 equiv or more of HMPA was added. One way to think about these species is as follows: In a classical 4-center dimer, coordination of two additional ligands like HMPA (or THF) to each lithium may be difficult, especially if the carbanion is sterically demanding. On the other hand, the isomeric triple ion allows easy tetrasolvation of the lithium counterion, and even the central electron rich lithium may be weakly solvated. This extra solvation can compensate for the loss of  $\text{C}^-\text{Li}$  coordination in the triple ion. Several di- and triorganosilyl-substituted methyllithiums formed triple ions, most notably **42-TI**, where the triple ion was a major constituent even in THF solution.<sup>34e,49</sup> Enolates also formed minor amounts of triple ions with HMPA.<sup>43a,b</sup>



That the central lithium was still electrophilic could be demonstrated for the triple ion **41-TI**, where the  $^{15}\text{N}/^6\text{Li}$  doubly enriched compound showed a triplet for the lithium signal from coupling to two  $^{15}\text{N}$  nuclei,  $J_{^{15}\text{N}^6\text{Li}} = 1.6$  Hz.

Many  $\alpha$ -thiomethylithium reagents, particularly chelated ones, also formed triple ions. One of the best characterized of these is **43**.<sup>47</sup> The two signals at  $\delta_{\text{Li}}$  5.0 and 5.3 correspond to two diastereomeric triple ion structures, one of which is shown in Figure 12. In the  $^7\text{Li}$  NMR spectra of the  $^{13}\text{C}$  labeled compound these are triplets, showing that two carbons are bonded to lithium. Here also, the central lithium is still chelated to the pyridyl nitrogens as indicated by the unusual downfield

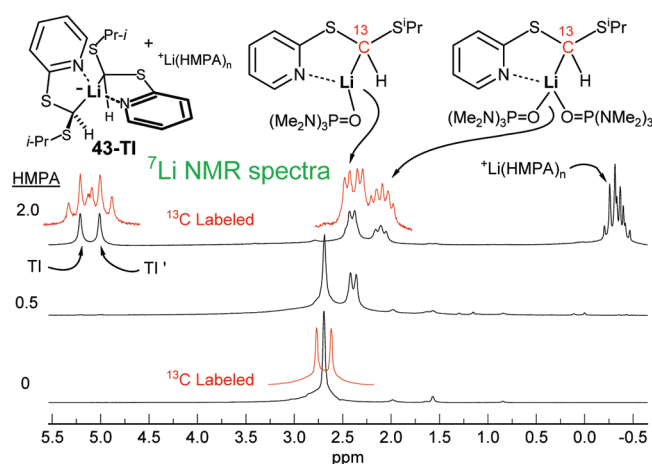


**Figure 12.** HMPA titration of **43**. The red inserts are  $^7\text{Li}$  NMR spectra of  $^{13}\text{C}$  enriched material.<sup>47</sup>

chemical shifts, characteristic of lithium coordinated to pyridyl groups. Related triple ions without such coordination appear at  $\delta_{\text{Li}}$  1.5–3.0.

Triple ions could well play important roles in the reactions of lithium reagents since they feature a strongly activated and less encumbered carbanion (compared to a 4-center dimer) as well as a Lewis acidic lithium cation. We were not able to study their reactivity, since in almost all cases they were in sufficiently rapid equilibrium with other species that even under optimum conditions direct study with our rapid-inject NMR (RINMR) apparatus (see below)<sup>50</sup> was not possible. The only exception was **42**, where the barrier for triple ion dissociation was  $>16$  kcal/mol.<sup>34e,51,52</sup> This chemistry is discussed in a separate section on RINMR below.

## ■ CHELATED ARYLLITHIUM REAGENTS

Coordination of lithium to nearby Lewis basic groups, both within the organometallic reagent and between it and the substrate, is a common design feature in organolithium chemistry. Chelation rationales have been especially common in explaining the rates and regioselectivities of metalation reactions (ortho-metalation) but have also been used to explain configurational stabilities, regioselectivities, and diastereoselectivities in reactions. At the time we became interested in this topic there was spectroscopic evidence in solution and considerable solid state X-ray crystallographic evidence for chelation by ether, amide, and other groups. However, of the many situations where chelation was proposed, only in a few cases was there direct evidence. It was assumed that any basic site capable of forming a 5- or 6-membered chelate was chelated, and the kinetic, stereochemical, and regiochemical consequences were interpreted in terms of such coordination. In hydrocarbon solvents it is almost guaranteed that any Lewis base available would become coordinated to an available lithium, but the situation was less clear in the more basic solvents like ether and THF in which lithium reagents are usually used.

We studied the solution structure and some reactivity effects of several types of organolithiums with chelating groups. Our work with  $\alpha$ -thio/ $\alpha$ -silyl-substituted methyllithiums with pendant amine and ether groups will be summarized in a separate section below. Here we discuss aryllithium reagents, such as *o*-(dimethylaminomethyl)phenyllithium **44**, the poster-



child of chelation induced metalation first reported by Hauser.<sup>53</sup>

Our study began with a thorough investigation of the solution structure of phenyllithium itself, and several alkyl-substituted derivatives as models.<sup>42</sup> In THF PhLi is a mixture of monomer and dimer,<sup>24b</sup> in ether a mixture of dimer and tetramer. HMPA and PMDTA converted PhLi to monomers. Amazingly, 12-crown-4 had no effect on aggregation state, although large increases in reactivity were noted.

Compound **44** had been examined several times, with conflicting results. We performed a thorough NMR study of **44** and a series of related structures using <sup>15</sup>N- and <sup>6</sup>Li-enriched material.<sup>30c,b,d,c</sup> At low temperatures in THF, **44** is dimeric and forms a mixture of three chelation isomers (A–C), one of the earliest examples of such isomerism (Figure 13). Very striking

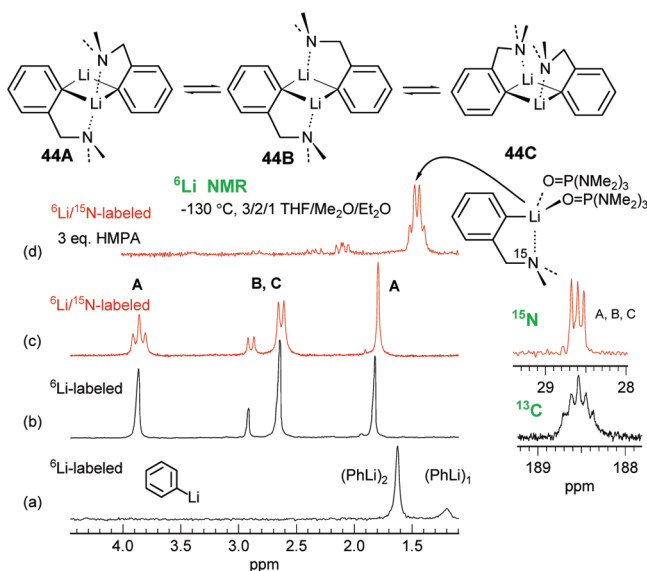
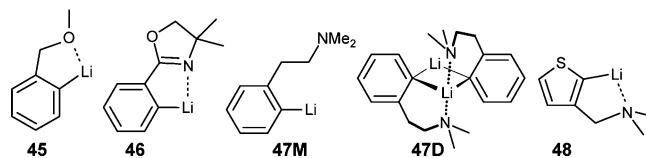


**Figure 13.** (a) <sup>6</sup>Li NMR spectrum of <sup>6</sup>Li-PhLi in THF. (b) <sup>6</sup>Li and <sup>13</sup>C NMR spectra of <sup>6</sup>Li-**44**.<sup>42</sup> (c) <sup>6</sup>Li and <sup>15</sup>N NMR spectra of <sup>6</sup>Li,<sup>15</sup>N-**44** in THF/Me<sub>2</sub>O/Et<sub>2</sub>O. The triplet for A and the doublets for the B and C peaks are due to Li–N coupling. An assignment of B and C was not made. (d) <sup>6</sup>Li NMR spectrum of <sup>6</sup>Li,<sup>15</sup>N-**44** with 3 equiv of HMPA added. The apparent quartet is from nearly equal couplings between <sup>6</sup>Li and the coordinated <sup>15</sup>N and <sup>31</sup>P.<sup>30c,d</sup>

was the observation that the dimer of **44** is much more stable, both kinetically and thermodynamically, than nonchelated models. Thus,  $K_{MD}$  ( $2 M \rightleftharpoons D$ ) was  $>17000 M^{-1}$  for **44**,  $1.7 M^{-1}$  for 2-ethylphenyllithium,<sup>30c</sup> and  $25 M^{-1}$  for PhLi at  $-135 ^\circ C$ .<sup>42</sup> Similar effects were seen for the ether analogue **45**.<sup>30d</sup> The origin of these large changes in  $K_{MD}$  is not well understood. The chelating amines TMEDA and PMDTA were unable to disrupt the chelation or cleave the dimer, although both were able to displace THF. The more potent cosolvent HMPA did convert dimers to monomers, but chelation was not disrupted (Figure 13d). The *o*-lithio oxazolines **46** were also chelated with higher dimerization constants than expected.<sup>30f</sup>

The 6-ring chelated analogue **47** also showed very interesting behavior: the compound was marginally more dimerized than model systems ( $K_{MD} = 219 M^{-1}$  at  $-137 ^\circ C$ )<sup>30c</sup> but the NMR spectra of <sup>15</sup>N labeled material showed that the monomer **47M** was not chelated, whereas the dimer **47D** was. That these and other behaviors reflect a close balance between external and

internal solvation was shown by studies of the analogous thiophene system **48** and its ether analogue, which in sharp contrast to **44** and **45** showed little difference in  $K_{MD}$  between either the amine or the ether chelated and their nonchelated analogues.<sup>30e</sup>



## ORGANOLITHIUM STEREOCHEMISTRY

Most vinyl, cyclopropyl, and  $\alpha$ -alkoxy lithium reagents are configurationally stable.  $\alpha$ -Amido-substituted lithium reagents can be prepared in enantioenriched form but racemize readily.<sup>54</sup> Alkylolithiums and others with  $\alpha$ -substituents such as phosphinyl, thiol, sulfinyl, and sulfonyl are quite configurationally labile, and nonequilibrium ratios of enantiomers or diastereomers can only be produced at very low temperature, if at all. Their inversion processes can best be studied by DNMR methods using diastereotopic labels. One limiting mechanism for organolithium reagent epimerization is a bimolecular associative process through intermediate **49** or **50** (Figure 14). An alternative ion pair dissociation process via

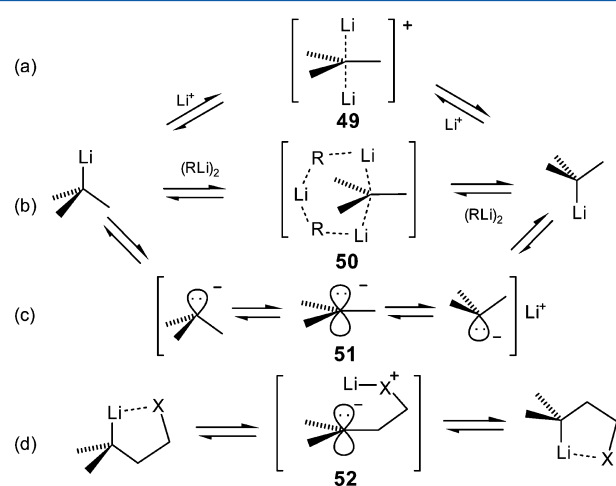
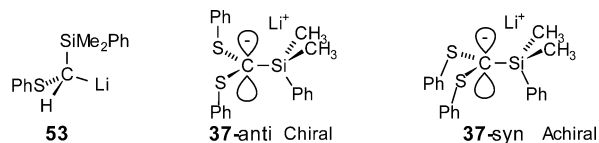


**Figure 14.** Limiting mechanisms for lithium reagent configurational inversion: (a), (b) Associative: lithium catalysis by free lithium cation or a RLi aggregate. (c) Dissociative: ionization to an SIP. (d) Conducted tour of a chelated lithium reagents.

**51** has been frequently proposed since polar solvents usually accelerate racemization. It had not been directly testable since the ion pair status of most lithium reagents was not known. A third process, dubbed a “conducted tour” mechanism by Cram,<sup>59a</sup> in which the lithium cation is passed from the carbanion center to a basic group (X) on the molecule to give intermediate **52**, which then transfers it to the other face without having to pay the energetic cost of a formal ion separation.

The mechanisms outlined in Figure 14 are in principle experimentally distinguishable in DNMR experiments. We examined a variety of  $\alpha$ -(aryltio)methylolithium reagents bearing diastereotopic labels, some with chelating groups. One carefully studied system was **53**. In sharp contrast to expectations based on ion-pair dissociation mechanisms for

stereochemical inversion, we found that the barrier to inversion increased when the CIP was converted to an SIP by addition of HMPA. In 3:2 THF/ether,  $\Delta G_{-100}^{\ddagger}$  was 8.0 kcal/mol for the CIP, which increased to 9.1 kcal/mol for the SIP, a factor of ca. 20 slower.<sup>12a</sup> Significant planarization of the SIP was indicated by an increase in  $^1J_{\text{CH}}$  from 132 to 148 Hz, and  $^1J_{\text{CSi}}$  from 75 to 106 Hz accompanying ion separation (other similar reagents also became more planar upon ion separation<sup>12b</sup>). We concluded that the energy barrier to racemization had little to do with the inversion process at the chiral carbon. Rather, the significant barrier was rotation around the C–S bond, related to hyperconjugative interactions between the carbanion lone pair and the C–S antibonding orbital ( $n-\sigma^*$ ), which become stronger in the SIP.<sup>55</sup>



Strong support for this notion was provided by the observation that **37**, which is largely a SIP in THF (Figure 9a), was chiral, with diastereotopic  $\text{SiMe}_2$  groups up to  $-12^\circ\text{C}$ ,  $\Delta G_{-12}^{\ddagger} = 13.3$  kcal/mol, even higher than for **53**.<sup>12a</sup> This anion is chiral *only* if there is slow rotation around the C–S bond and the two phenyl groups are anti (**37-syn** is achiral), but *not* if inversion is slow at the carbanion center and rotation is fast. In fact, the high barrier to racemization of **37** and other observations indicate that the racemization of the SIP of **53** might be proceeding through the CIP, the complete reverse of the process in Figure 14c!

The behavior of chelated analogues of these reagents was significantly different and will be detailed below in the section on Chelated Aryllithium Reagents.

Additional evidence for the importance of  $n-\sigma^*$  interactions in the stereochemistry of  $\alpha$ -thio and  $\alpha$ -seleno carbanions was provided by observations made during the cleavage of the selenoketals **54** and **55** by alkyllithium reagents (Li/Se exchange).<sup>11,56a</sup> The bis(phenylseleno)ketal **54** undergoes highly selective cleavage of the axial PhSe group. If the cleavage is done in the presence of trimethylsilyl chloride a kinetic ratio of silanes could be trapped, favoring the axial isomer by 98/2. The thermodynamic ratio of lithium reagents was 93/7. In sharp contrast, the equatorial C–Se bond is almost exclusively cleaved in the cyclic selenoketal **55**, leading to a 3/97 ratio of silanes with an in situ quench (Figure 15). The thermodynamic ratio also favored the axial lithium reagent (sequential quench).

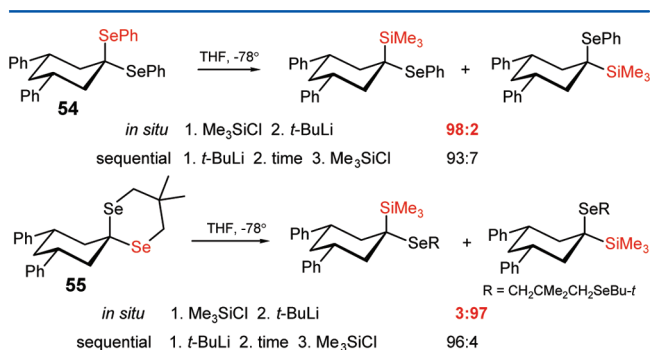
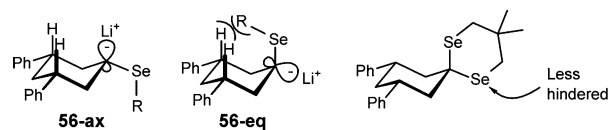
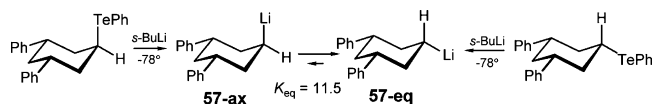


Figure 15. Stereochemistry of Li/Se exchange of selenoketals.<sup>11</sup>

A reasonable explanation for this remarkable switch in stereochemistry of the Li/Se exchange is as follows: The thermodynamic preference for axial lithium reagent is a consequence of a more effective  $n-\sigma^*$  overlap in the axial (**56-ax**) than in the equatorial (**56-eq**) lithium reagent. Attack at the less hindered equatorial PhSe in **54** suffers from the same problem in achieving optimal  $n-\sigma^*$  overlap (steric inhibition of hyperconjugation) in the transition state leading to the lithium reagent or to the intermediate ate complex, as illustrated for **56-eq**, leading to preferred attack at the axial selenium. In contrast, for cyclic selenoketal **55** the two seleniums are stereoelectronically equivalent, and the kinetically preferred attack by  $t\text{-BuLi}$  is at the sterically less encumbered equatorial selenium by a 44/1 margin, leading to the less stable equatorial reagent.



An examination of the barrier to stereoinversion of a cyclohexyllithium reagent (**57**) suggested an aggregate-based mechanism (Figure 14b). The rate of inversion was increased when THF was replaced by  $\text{Et}_2\text{O}$ , and decreased when DME or PMDTA was added to THF solutions. PMDTA favors monomeric structures<sup>20c</sup> and can actually be used to probe the stability of dimeric reagents.<sup>30c,d,f,42,43b</sup> We presume the rate-retarding effect is due to suppression of a dimer-based inversion mechanism (e.g., via **50**, Figure 14b).<sup>57</sup> In contrast TMEDA, which complexes well with dimers, has no effect on the inversion rate. The two isomeric cyclohexyllithium reagents could be effectively prepared only by a Li/Te exchange.<sup>56b,58</sup> Other methods failed.



## CHELATED ALKYLITHIUM REAGENTS

An extensive study of numerous methylithium reagents bearing anion-stabilizing substituents like  $\text{R}_3\text{Si}$ , RS, Ar, vinyl or alkynyl on carbon, revealed several significant differences among those reagents with or without pendant chelating groups such as pyridyl, alkoxy, amino, and amido.

**Ion Separation.** For those reagents where HMPA can induce ion separation (i.e., two or more anion-stabilizing groups such as **58–62**, Figure 16) significantly more HMPA was needed for 5-ring chelated reagents than for nonchelated analogues.<sup>30a,b,36b,c,40a</sup> The  $^7\text{Li}$  and  $^{31}\text{P}$  NMR spectra in Figure 16a,b illustrate this very different behavior: for **58** the formation of SIP ( $\text{R}^-/\text{LiH}_3^+$ ) is nearly complete at 2 equiv of HMPA, and only a small amount of the mono-HMPA coordinated CIP  $\text{R-LiH}_1$  remains. For **61**, on the other hand, mostly CIPs are seen ( $\text{R}^-\text{LiH}_1$ ,  $\text{R}^-\text{LiH}_2$ ). Only a small amount of SIP is detected ( $\text{R}^-/\text{LiH}_4^+$ ), and this can be assigned to the formation of triple ion ( $\text{R}_2\text{Li}^- \text{Li}^+$ ) and not to true SIP. Even excess HMPA causes only insignificant ion separation. Also interesting is the  $^{31}\text{P}$  NMR spectrum of **61**, where the bis-HMPA complex is the main species present. There are two  $^{31}\text{P}$  signals (marked  $\text{R-LiH}_2$ ), corresponding to diastereotopic HMPA resonances of the complex. Clearly, the prochiral Li center is configurationally stable on the NMR time scale. Similar diastereotopic  $^{31}\text{P}$  signals

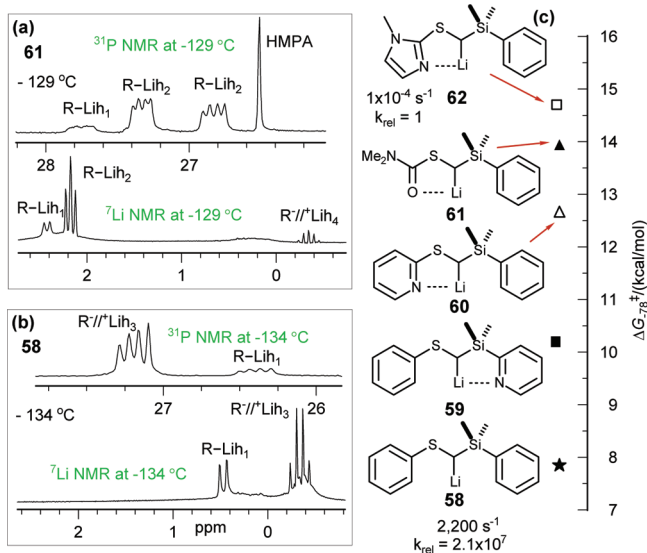


**Figure 16.** (a, b)  $^7\text{Li}$  and  $^{31}\text{P}$  NMR spectra of **58** and **61** at 2 equiv of HMPA. (c) Configurational inversion barriers at  $-78^\circ\text{C}$  for one unchelated (**58**) and four chelated (**59–62**) S,Si-substituted methylithium reagents in 3:2 THF/ether.

have been seen for a number of related alkylolithium reagents<sup>40a</sup> as well as for the *N*-methyl-*N*-isopropyl analogue of the aryllithium **44**.<sup>30c</sup> Even the  $^{31}\text{P}$  NMR signals of diastereomeric solvates can be detected, differing only in the stereochemical arrangement of two different coordinated solvents.<sup>30b</sup>

**Reactivity.** When the  $\text{S}_{\text{N}}2$  reactivity of chelated and nonchelated reagents was compared, the chelated ones were typically 1–3 orders of magnitude less reactive. For example, the relative rate of methylation of **63** vs the chelated analogues **64** and **65** was 2/1 in THF/HMPA at  $-78^\circ\text{C}$  (i.e., the inherent reactivity of the SIPs is nearly the same), but in THF **63** is 26 times more reactive than **64** and 100 times more reactive than **65**. The effect was larger for the more strongly chelated reagent, as determined from HMPA titrations. This can be directly ascribed to the effect of chelation in reducing the equilibrium concentration of the SIP (Figures 10 and 16), which we believe is the reactive nucleophile in most such reactions.<sup>36c</sup>

	<b>63</b>	<b>64</b>	<b>65</b>
$k_{rel}$ (MeI/THF)	1	1/26	< 1/100
$k_{rel}$ (MeI/HMPA)	1	0.5	0.5

Even larger reactivity effects were seen for bis-chelated systems. Comparison of  $(\text{PhS})_2\text{CHLi}$ ,  $(2\text{-PyS})\text{PhSCHLi}$ , and  $(2\text{-PyS})_2\text{CHLi}$  gave relative alkylation rates with MeI of 1.0, 1/400, 1/18000.<sup>36b</sup>

**Racemization.** The configurational stability of chelated S- and Si-substituted alkylolithium reagents is usually significantly higher than those of model compounds.<sup>30a,36c</sup> Figure 16c gives the racemization barriers of a few members of this series, measured by DNMR line shape analysis of the diastereotopic  $\text{SiMe}_2$  groups. They range from 8 to 15 kcal/mol at  $-78^\circ\text{C}$ , corresponding to a  $2.1 \times 10^7$  faster inversion rate for the unchelated (**58**) vs the most strongly chelated structure (**62**). The inversion barriers qualitatively follow the strength of

chelation, as determined by the HMPA equivalents needed to cause ion separation (see Figure 10). Both a “clamping” effect, holding the lithium more tightly and preventing inversion,<sup>54a</sup> or a “conducted tour”<sup>59</sup> effect (Figure 14d),<sup>54b</sup> where the chelating group provides a low energy path to shuttle the lithium from face to face of the carbanion have been proposed. Apparently the former effect predominates here.

When inversion does occur, it seems to proceed by the “conducted tour” mechanism, as shown by a DNMR study of the chelated reagent **66** (Figure 17).<sup>30a</sup> For this compound the

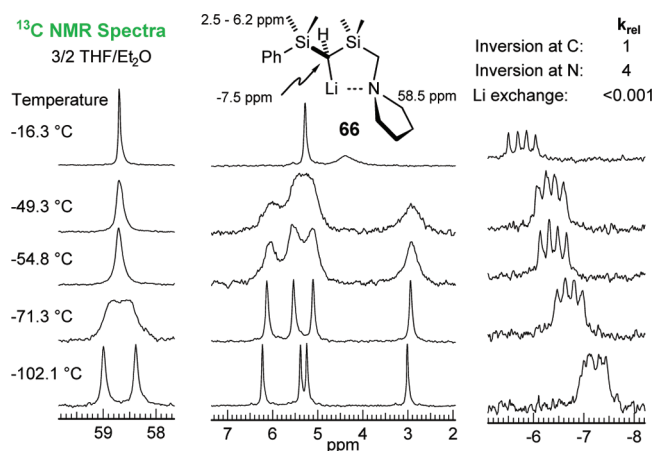


**Figure 17.** Variable-temperature  $^{13}\text{C}$  DNMR study of intramolecular processes in **66** in 3:2 THF/ether.<sup>30a</sup>

rate of inversion at the carbanion center can be measured from line shape analysis of the  $\text{SiMe}_2$  groups ( $\delta$  5) and intermolecular exchange of  $\text{Li}^+$  by loss of the C–Li coupling ( $\delta$   $-7$ , 1:1:1:1 quartet from coupling to the spin 3/2 nucleus  $^7\text{Li}$ ). No loss of coupling was detected to  $-16^\circ\text{C}$ , so inversion is at least 1000 times as fast as intermolecular  $\text{Li}^+$  exchange. These data speak strongly for a high preponderance of a “conducted tour” mechanism (Figure 14d), since the associative and dissociative mechanisms require intermolecular Li exchange at rates comparable to configurational inversion. The experiment also measures the rate of N–Li decoordination and inversion at nitrogen by DNMR coalescence of the C–N carbons ( $\delta$  59), which is about 4x as fast as inversion at carbon.

## REGIOSELECTIVITY OF RLi ADDITION TO ENONES

The ability to easily and reliably determine and manipulate the ion pair status using HMPA titration studies allowed us to test some mechanistic hypotheses involving the CIP/SIP dichotomy. One interesting and useful example is the report by Brown and Yamaichi<sup>60</sup> that the competition between direct (1,2) and conjugate (1,4) addition of 2-lithio-1,3-dithiane to enones is strongly affected by the presence of HMPA. Reactions in THF give 1,2-addition, whereas addition of HMPA caused an almost complete switch to 1,4-addition. There are several possible mechanisms for such an effect. HMPA might accelerate the equilibration of 1,2- to 1,4-adducts by speeding up the retro-1,2 addition, it might encourage SET mechanism by creating more electron-rich carbanions, or changes in the carbanion structure might directly affect the regioselectivity. A proposal was made by Bryson<sup>61a</sup> and Cohen<sup>61b</sup> that CIP species underwent 1,2 addition while SIP species favored 1,4 addition, supported by observations that lower temperatures and the presence of HMPA (both known to

favor SIP over CIP) led to more 1,4-addition. Since the ion-pair status of the lithiodithiane in these solutions was unknown at the time, we felt that an examination of this question would be fruitful.

Indeed, we found that for a number of  $\alpha$ -thiomethyl lithium reagents the switch from 1,2-adducts to 1,4-adducts paralleled the increase in the measured fraction of SIP, but was not directly proportional to it. Rather the switch to 1,4-addition substantially preceded the CIP to SIP conversion (Figure 18).<sup>40</sup>

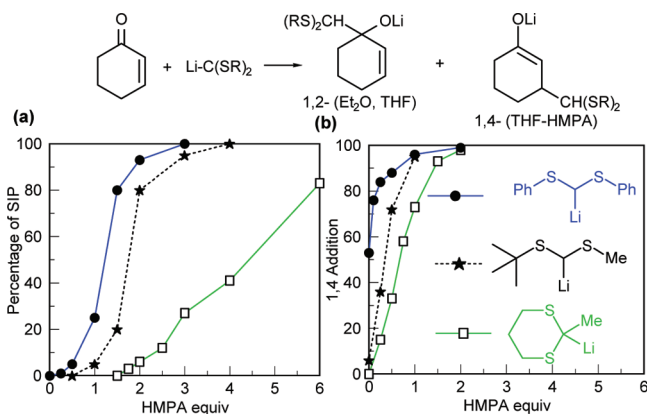
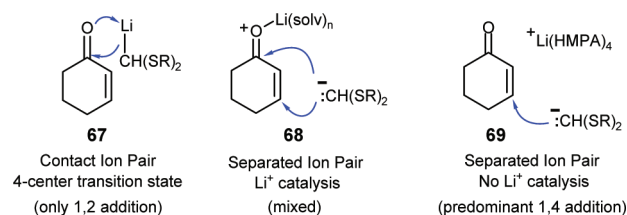


**Figure 18.** Effect of HMPA on (a) ion separation and (b) ratio of 1,2 to 1,4 addition to cyclohexenone (in THF,  $-78\text{ }^{\circ}\text{C}$ ).<sup>40</sup>

Thus, this was a Curtin–Hammett situation, where small equilibrium fractions of the SIP formed at low equivalents of HMPA dominated the process long before they were the main species because of their much higher reactivity. For some reagents ( $(\text{PhS})_2\text{CHLi}$ ), substantial 1,4-addition already occurred in THF (Figure 18b). Such reactions switched entirely to 1,2-addition in weaker coordinating solvents like diethyl ether or ether–hexane.

A careful examination of the diastereomer ratios of both the 1,2 and the 1,4 adducts for several reactions where one or both the lithium reagent and the enone were chiral, showed that three distinct processes could be distinguished. Under all conditions, the diastereomer ratio of the 1,2-adducts was essentially constant, pointing to a uniform mechanism, the 4-center process illustrated by **67**. As the solvent polarity was increased from ether to THF and then to THF–HMPA the 1,4-adduct diastereomer ratio varied little until the lithium cation became coordinated to HMPA, when substantial changes in both the regioisomer and diastereomer ratios occurred for some systems. We interpret these and other observations in terms of two processes which lead to 1,4-adducts. In THF the separated lithium cation is able to act as a Lewis acid, as in **68**. This path forms mostly 1,4 adducts, but also forms some 1,2. Once the  $\text{Li}^+$  is sufficiently encumbered by HMPA the enone can no longer compete for  $\text{Li}^+$ , and an uncatalyzed highly 1,4-selective process illustrated by **69** with different diastereoselectivity becomes competitive. One of the observations in support of a switch from **68** to **69** was that addition of HMPA caused large decreases in the rate of formation of the 1,4-adduct, in one case by at least a factor of 1000 at  $-78\text{ }^{\circ}\text{C}$ .<sup>40</sup>

**Metalated Nitrile Enone Additions.** Our consideration of the 1,2 vs 1,4 additions next led to an examination of metalated nitrile reactions with enones, specifically lithioarylacetonitriles. These had been extensively studied, and several attractive



rationales for the changes in selectivity had been proposed. These included aggregate effects, where the monomer gives 1,2-product (as in **67**), and the dimer gives 1,4-products through an extended transition state.<sup>62</sup> Also proposed were hard and soft acid base (HSAB) considerations: 1,4-addition is favored by soft and 1,2 by hard anions (CIP soft, SIP hard;<sup>63a</sup> delocalized anions soft, more localized anions hard<sup>63b,64</sup>).

By careful examination of substituted lithiophenylacetonitriles with benzylideneacetone at low temperatures in THF we were able to establish that the kinetic products in all but one special case were 1,2 adducts (**70**, Figure 19), with at least 50:1

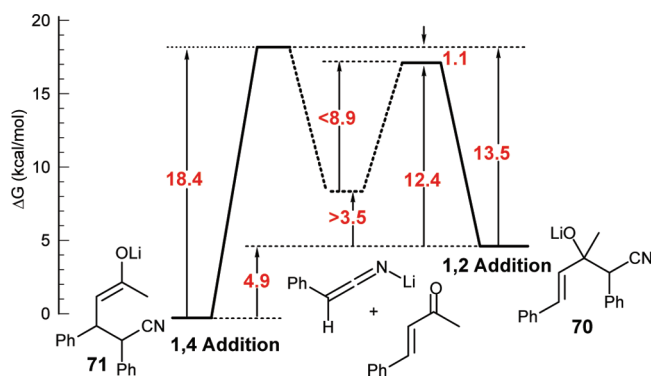


**Figure 19.** Energy level diagram for the lithiophenylacetonitrile–benzylideneacetone system in THF.<sup>65</sup>

selectivity, and that the 1,4-adducts (**71**) were formed by reversal of the 1,2-addition, and formation of the more stable 1,4 adduct. Thus, all of the very plausible arguments for kinetic preferences based on aggregation or HSAB principles do not apply. Estimates for the various rates were made by watching the equilibration of purified 1,2 adduct diastereomers (rate of retro-1,2,  $\Delta G^\ddagger = 12.4$  kcal/mol), observing the isomerization of 1,2 to 1,4 adducts ( $\Delta G^\ddagger = 13.5$  kcal/mol), and measuring the rates of retro-1,4 addition by crossover and trapping experiments ( $\Delta G^\ddagger = 18.4$  kcal/mol). The only process that could not be measured was the initial 1,2 addition, which was too fast for laboratory time scale experiments even at  $-100\text{ }^{\circ}\text{C}$ , with  $\Delta G^\ddagger < 8.9$  kcal/mol. The RINMR apparatus, see below, might have helped with this but was not yet available. We believe this to be the first semiquantitative experimentally determined energy profile of this important class of reactions (Figure 19).<sup>65</sup> From the kinetic experiments we estimate that the 1,4-adduct **71** is 5 kcal/mol more stable than **70**.

This work also revealed an example of a mixed aggregate playing an important role in a reaction. It was observed that the 1,2 to 1,4 isomerization had a fast phase, up to 50% conversion, followed by a second phase approximately 1/20 as fast (the barrier shown in Figure 19 is for the fast phase). We reasoned that the retro-aldol for the 1,2-alkoxide homoaggregate (presumably the dimer (**70**)<sub>2</sub>) was much faster than for the alkoxide–enolate mixed aggregate (**70**·**71**) present at 50%

conversion and gathered some evidence in support of this explanation.

**Enolate Structures.** In connection with these studies it became important to understand the solution structures of enolates, where existing methods<sup>2c,66</sup> were difficult and not always reliable. The HMPA titration of cyclopentanone and cyclohexanone lithium enolates could only be interpreted in terms of tetramer structures, other studies had indicated aggregation states from dimers to pentamers. An extensive examination of several other enolates showed that the HMPA titration method was effective in defining aggregation states. Unhindered enolates were tetramers, more hindered ones having delocalizing substituents (e.g., Ph) at the enolate carbon were dimers in THF.<sup>43a,b</sup> For some systems various mixing experiments, recently highlighted by the Collum group,<sup>2c</sup> were used to firmly establish aggregation states.

When enolates were prepared under “lithium deficient” conditions, either by addition of HMPA, cryptand[2,2,1], or other strong Li-coordinating bases, or by mixing lithium enolates with metal-free enolates formed by deprotonation with the Schwesinger P4 base, novel species not previously detected were formed (Figure 20). At a 1:1 ratio of Li and P4 enolates triple ions (RO)<sub>2</sub>Li<sup>-</sup> M<sup>+</sup> (72, M = Li(HMPA)<sub>4</sub><sup>+</sup> or P4H<sup>+</sup>) were formed, and at 1:2 ratio “quadruple ions” of the (RO)<sub>3</sub>Li<sup>2-</sup> 2M<sup>+</sup> type (73).<sup>43a,b</sup>

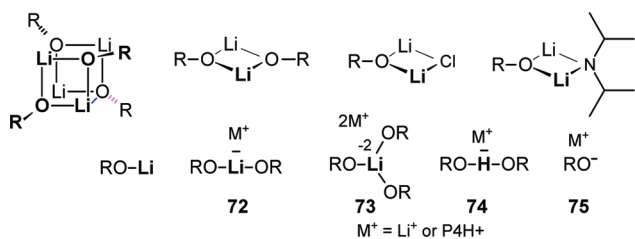


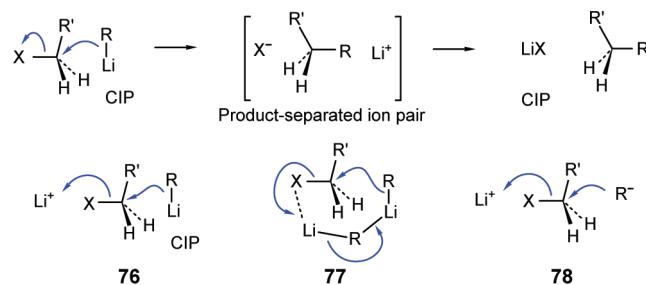
**Figure 20.** Some aggregates and mixed aggregates for enolates of acetophenone, dibenzyl ketone, and related structures characterized spectroscopically (R = vinyl groups).<sup>43</sup>

The conjugated lithium-free enolates formed by deprotonation of dibenzyl ketone with P4 base formed hydrogen bridged dimers (RO–H–OR– P4H<sup>+</sup>, 74) as thermodynamically stable species at 0.5 equiv of base.<sup>43d</sup> This low-barrier hydrogen bond is strong enough to pay the energetic cost of the keto–enol tautomerization. From DNMR exchange experiments between enolate 75 and the H-bonded species 74 we estimate the bond strength to be ca. 11 kcal/mol. Unfortunately, their interconversion is too fast for direct study by our RINMR techniques, so their contribution to the chemistry of enolates is not known. The NMR properties of H-bonded dimers are very similar to those of 4-center lithium enolate dimers, suggesting similar amount of negative charge in both species. Enolate reactivity is discussed further in the RINMR section of this paper.

## REACTION OF HALIDES AND EPOXIDES

The ability to readily identify the ion-pair status of commonly used organolithium reagents allowed us to probe the role of ion pairs in the mechanism of their substitution and addition reactions. When strongly ion-paired species are the nucleophiles in S<sub>N</sub>2 reactions, there is a conundrum which Cram in another context elegantly called the “product-separated ion-pair” problem.<sup>59b</sup> Since the nucleophile is coordinated to the

lithium cation, and there is a strong preference for backside attack, the transition state must involve substantial charge separation, with the departing anion emerging separated from the lithium cation by the product.



This problem can be avoided by a number of molecular strategies: an extraneous free lithium cation (or another R–Li molecule) can assist in the departure of the leaving group in a termolecular process (76), lithium aggregates could form a Li–C–Li–C chain to “conduct” the charge from front to rear of the product (77), or the Li–R could predissociate to release the cation as a SIP (78). The latter mechanism has the additional feature than an enormously more reactive free carbanion would be the nucleophile instead of the C–Li species.

To probe this effect we examined the kinetics of S<sub>N</sub>2 reactions in THF and THF–HMPA of sulfur-stabilized lithium reagents with typical S<sub>N</sub>2 substrates: alkyl, allyl and benzyl halides, aziridines and epoxides.<sup>67</sup> We expected two opposing effects of a polar cosolvent. The increased degree of ion pair separation will replace a weakly nucleophilic R–Li CIP with a very much more reactive R<sup>-</sup>/Li<sup>+</sup> SIP. On the other hand, coordination of HMPA to lithium will decrease the ability of Li<sup>+</sup> to facilitate the departure of the leaving group. The latter effect should be especially important in epoxide openings, in which the leaving group is very basic (lithophilic), and less so or absent in halide or sulfonate displacements. Our study involved three lithium reagents: bis(3,5-bistrifluoromethylphenylthio)methylithium 79, a SIP in THF,<sup>51</sup> bis(phenylthio)methylithium 80, a weak CIP (half ionized at 1 equiv of HMPA, Figure 10, 18a),<sup>40b</sup> and 2-lithiodithiane 81, a strong CIP (half ionized at 4.5 equiv of HMPA).<sup>41d</sup> All three species are monomeric. A summary of some rate data for reaction with butyl halides, propylene oxide, and *N*-tosylpropyleneaziridine are summarized in Figure 21, which shows the changes in rate constants caused by addition of HMPA.<sup>67</sup>

The very striking difference between the three lithium reagents can be rationalized as follows: all reactions with alkyl bromides, chlorides and iodides occurred by one mechanism: the CIP R–Li species is in equilibrium with the SIP, which reacts with the halide without any assistance from the lithium cation. The change caused by addition of HMPA was solely determined by the relative increase in concentration of the SIP. Since 79 is already almost fully separated in THF, HMPA has no effect on the rate of halide substitution. For 80, the rate increase was a factor 300–400 for all halides tried (*i*-BuBr, *n*-BuBr, *n*-BuCl, allyl-Cl, *i*-PrI, BnCl), so 0.3% of 80 is SIP in THF. For 81, the rate increased by a factor of 5900000. The dynamic range for 81 was too large to study a variety of halides, but competition experiments between pairs of halides showed that here also there was no change in relative rate when HMPA (or other ion-separating cosolvents such a DMPU) were added. Thus, the same species (the free carbanion) was always the active nucleophile. It is the strong propensity for anions of this

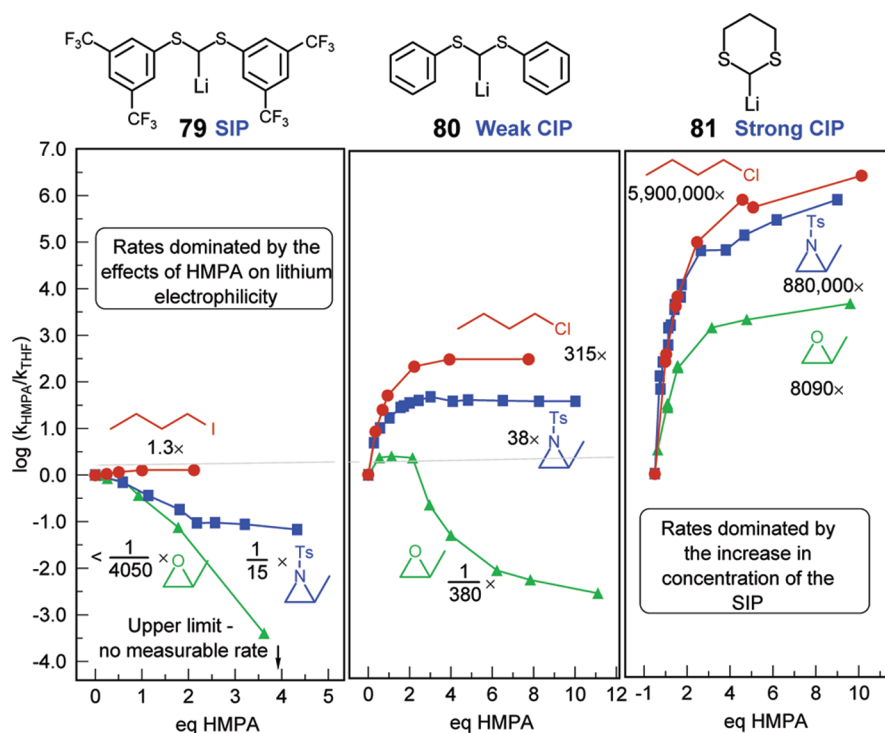
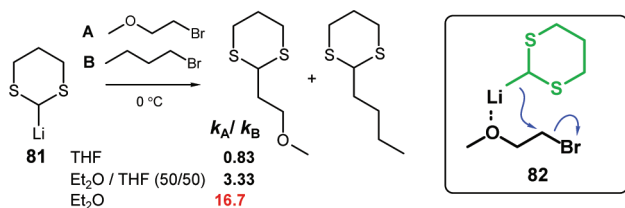


Figure 21. Effect of HMPA on organolithium reagent  $S_N2$  substitutions rates in THF at  $-78\text{ }^\circ\text{C}$ .<sup>67</sup>

type to react as SIP which has made asymmetric alkylation using chiral ligands for lithium difficult to achieve.<sup>56c</sup> The base is complexed to the separated lithium cation, which interacts weakly at the transition state.

We did find one likely exception to the SIP mechanism. When the relative reactivity of butyl bromide and 2-methoxyethyl bromide with **81** was measured in THF or with a variety of polar cosolvents (HMPA, DMPU 12-crown-4, PMDTA) the ratio was constant. However, when solvent polarity was reduced, going to ether/THF and then pure ether, the bromoether became much more reactive than BuBr. Iodides and chlorides show nearly identical behavior. We interpret these results in terms of the coordinated structure in transition state **82**.<sup>36d</sup> This process comes into play when the fraction of SIP becomes vanishingly small and competition for the lithium by solvent is diminished, allowing this complex-induced proximity effect (CIPE) to operate.<sup>68</sup>



The situation with epoxides as electrophiles was very different. Here also the SIP was the reactive species, but the precipitous drop in rate for **79** as HMPA was added indicated a pronounced Lewis acid assistance in the  $S_N2$  reaction by the lithium counterion in THF, which was reduced and eventually eliminated as the  $\text{Li}^+$  was sequestered by HMPA. For **80** the rate increased initially (more SIP, still some  $\text{Li}^+$  assistance) but then dropped to a fraction of the THF rate. The contrast between alkyl halide and epoxide reactions with **80** is illustrated in Figure 22. For the dithiane **81**, HMPA still caused substantial

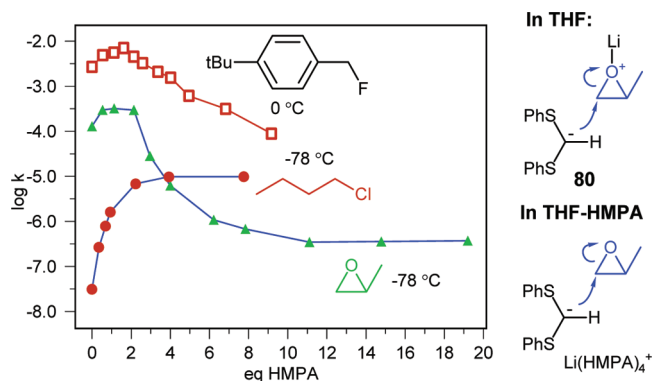


Figure 22. Different kinetic behavior of  $S_N2$  substitution of chlorides, fluorides, and epoxides with **80** on addition of HMPA (THF,  $-78\text{ }^\circ\text{C}$ , fluoride at  $0\text{ }^\circ\text{C}$ ).<sup>36d,67</sup>

rate acceleration (8090x) but much less than for the halides - the loss of  $\text{Li}^+$  assistance partially offsets the increase in SIP concentration. Interestingly, the behavior of fluoride as a leaving group with **80** is similar to that of epoxide (Figure 22). Thus, there is significant Lewis acid assistance to fluoride departure in the  $S_N2$  substitution, which has also been seen in other contexts.<sup>2d,23</sup>

The  $S_N2$  openings of aziridine show behavior intermediate between that of epoxides and halides: the level of lithium assistance is smaller, consistent with a less basic and more hindered leaving group ( $\text{p}K_a: \text{H}-\text{Cl} \ll \text{H}-\text{NTsR} < \text{H}-\text{OR}$ ).

**Take-Home Lesson.** These studies show that the interaction of HMPA with organolithium reagents is complex, and the behavior not always straightforward. Although HMPA and analogues like DMPU have a well-deserved reputation for activating the nucleophilic properties of lithium reagents, HMPA can also severely retard reactions by reducing  $\text{Li}^+$

activation. It is worthwhile to understand the opposing effects of HMPA in organolithium chemistry.

## OUTMANEUVERING THE CURTIN–HAMMETT PRINCIPLE: RINMR

The studies above, and indeed almost all kinetic studies of lithium species ever reported (a few exceptions<sup>2e,69a,70</sup>), were performed under Curtin–Hammett conditions. The individual aggregates, mixed aggregates, and their solvates (not to mention alkoxides and other impurities) were in rapid equilibrium, and their mechanistic involvement could only be indirectly teased out from kinetic orders, line curvatures, product ratio changes, isotope effects, etc. There is a very good reason for this. To operate under non-Curtin–Hammett conditions the activation energies for the reaction being studied must be lower than those for species interconversion; i.e., the reaction  $\Delta G^\ddagger$  must be  $>13$  kcal/mol at  $-78$  °C and  $>18$  kcal/mol at  $0$  °C for half-lives greater than a few seconds. Yet almost all measured barriers for interconversion of organolithium aggregates and ion pair structures are well under 13 kcal/mol, and most are under 10 kcal/mol, especially in ether solvents. Figure 23 gives some barriers we measured by DNMR

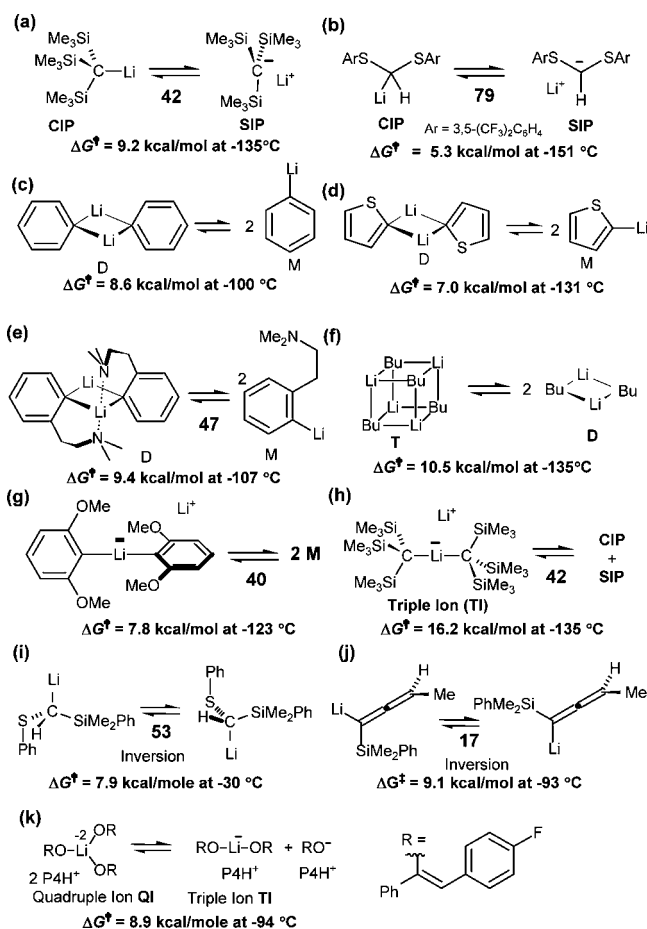


**Figure 23.** Some typical measured barriers of lithium species interconversion determined by DNMR methods: (a) CIP/SIP;<sup>34e</sup> (b) CIP/SIP;<sup>51</sup> (c) D/M;<sup>42</sup> (d) D/M;<sup>30e,34d</sup> (e) D/M;<sup>30c</sup> (f) T/D;<sup>50,56d,69b</sup> (g) TI/monomers;<sup>47</sup> (h) TI/monomers;<sup>34e,51</sup> (i) racemization;<sup>12a</sup> (j) racemization;<sup>27d</sup> (k) TI/quadruple ion.<sup>43a</sup> In all of these cases, both species are present in sufficient concentrations for individual study if under non-Curtin–Hammett conditions.

and rapid-inject NMR (RINMR) techniques. Many organolithium reactions are very fast and might well be measurable under non-Curtin–Hammett conditions so that information about reactive species would be direct and unambiguous. It is thus regrettable that kinetic studies were often forced to choose “tame” lithium reagents, unusual solvents (hydrocarbons), and/or especially unreactive substrates to get manageable rates.<sup>71</sup>

It is instructive to consider the  $\Delta G^\ddagger$  vs temperature plot in Figure 24 which defines the kinetic regions of interest. The

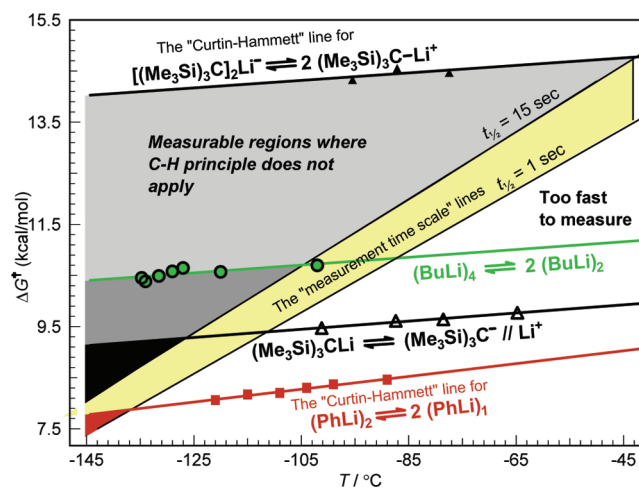


**Figure 24.** Curtin–Hammett limitations on measuring aggregate reactivity: the dimer and tetramer of *n*-BuLi, the monomer and dimer of PhLi and the TI, CIP, and SIP of  $(\text{Me}_3\text{Si})_3\text{C-Li}$  (42).

“Curtin–Hammett” lines are the rates of interconversion of the two species of interest (say two aggregates or two ion pairs). Any kinetic experiments with reactions whose activation energies (rates) are above these lines are subject to the Curtin–Hammett rule. Below the line, the rates of reaction of individual species can be measured independently. The further you are below the line the larger the flexibility and dynamic range of rate measurements. The time interval is also crucial and is given by the “measurement time scale” lines (15 and 1 s). Any rate below these lines (unshaded region) is too fast to measure on that time scale. As an example, the dark grey and black shadowed areas are suitable for performing experiments on mixtures of BuLi dimer and tetramer and observing their behavior independently. The red triangle defines this for PhLi monomer and dimer, requiring experiments below  $-135$  °C to detect individual reactivity, an almost hopeless situation. It is clear that measurements at very low temperature are crucial. Examination of Figure 23 shows that several of the interconversions might be inside the measurable region, and we undertook to explore this. In practice, it turns out that individual aggregates can have vastly different rates, so in real experiments some species may be reacting above the C–H line, others below it or even in the “too fast to measure” region.

McGarrity and Ogle<sup>69a</sup> performed the first RINMR experiments to directly address R–Li aggregate reactivity. They measured individual rates of *n*-butyllithium dimer and tetramer reactions at  $-85$  °C with 0.1 s time scale kinetics. This placed them just inside the upper-right corner of the “measurable region” triangle, leaving very little dynamic range between reaction of the dimer and dissociation of the tetramer.

The RINMR apparatus we constructed differs from the McGarrity one in that two pneumatically driven syringes were

externally mounted. This permits mixing with an external mechanical stirrer and allows operation at temperatures as low as  $-140\text{ }^{\circ}\text{C}$ , largely limited by solvent freezing and solubility issues. McGarrity ran all experiments above  $-90\text{ }^{\circ}\text{C}$ . The NMR pulse program controls raising, lowering, and actuating the syringes and stirrer. The instrument has a mixing time of just under 1 s (the fastest rate constants that can be measured are ca.  $1\text{ s}^{-1}$ ), and kinetic experiments can be run on time scales of 5 s to several hours. The two syringes allow a first injection to prepare a metastable species, and then a second to study its reaction with a substrate. The design and capabilities have been fully described.<sup>50</sup> This apparatus allowed us to do the first accurate measurements of the rates of reaction of *n*-BuLi aggregates with a number of electrophiles, the first kinetic studies of organolithium reagents reacting with aldehydes, esters and ketones, the first kinetic studies of LDA deprotonation of ketones and subsequent aldol reaction of the lithium enolates with aldehydes.

### RINMR STUDIES OF BUTYLLITHIUM REACTIVITY

By far the most widely used and best-studied organolithium reagent is *n*-BuLi. Although *n*-BuLi reacts with many functional groups, little is known about the rates of most of these reactions. Addition to carbonyl compounds has been studied in hydrocarbon solvents,<sup>72</sup> but in ethers the reactions are too fast. Only the slowest processes such as Li/Br exchanges,<sup>73,74</sup> difficult metalations,<sup>2g,75a</sup> or addition to weakly activated alkenes<sup>75b,76</sup> or imines<sup>2f</sup> have been studied. Because *n*-BuLi is one of the few lithium reagents with two coexisting aggregates for which non-Curtin–Hammett experiments are feasible (Figure 24), we initiated exploratory and some detailed studies, with a focus on the relative reactivity of the dimer and tetramer.<sup>50</sup> Most experiments were done at  $-130$  to  $-135\text{ }^{\circ}\text{C}$  in 3:1  $\text{Me}_2\text{O}/\text{THF}$ .

We were quickly able to divide electrophiles into several categories: those that were too slow to measure under non-Curtin–Hammett conditions ( $\text{Me}_3\text{SiCl}$ ,  $\text{PhCN}$ ,  $(\text{Me}_3\text{Si})_2\text{NH}$ ) and more reactive ones that did not react with *n*-BuLi tetramer but showed measurable rates ( $k < 2\text{ s}^{-1}$ ) with dimer ( $\text{Me}_2\text{C}=\text{O}$ ,  $\text{ArC}(\text{=O})\text{Me}$ ,  $\text{ArC}(\text{=O})\text{OMe}$ ,  $\text{ArC}(\text{=O})\text{NMe}_2$ , acetylene metalations,  $\text{MeSSMe}$ ,  $\text{PhSSPh}$ ,  $\text{EtSSEt}$ ). These were the ones we were most interested in (Figure 25). Then there were still more reactive ones that also did not react with tetramer but reacted in  $<1\text{ s}$  with dimer ( $\text{MeI}$ ,  $\text{PhCOCl}$ ), and the fastest ones that even reacted slowly with the tetramer ( $\text{PhCHO}$ ,  $\text{DMF}$ ). We should mention two other electrophiles that reacted rapidly with both dimer and tetramer: ROH species and  $\text{O}_2$ .

During this survey, we made the astonishing observation that BuLi dimer reacts with a tertiary amide about a factor of 7 faster than with a benzoate ester. In fact, the amide reacted at nearly the same rate as acetone (Figure 25). Any reasonable extrapolation from known rates, say of ester and amide hydrolysis, would predict amide rates to be many orders of magnitude slower than ester. This behavior must somehow be a consequence of the higher basicity of amide vs the ester or a rate-determining step that involves aggregate reorganization rather than carbonyl addition. Intensive efforts have not yet provided a clear explanation.<sup>36f</sup>

We chose for our first detailed study the metalation of trimethylsilylacetylene, which has favorable rates and well resolved  $^7\text{Li}$  NMR signals for starting material, intermediate, and product (Figure 26). The reaction with *n*-BuLi dimer is complete in less than 2 s at  $-130\text{ }^{\circ}\text{C}$ . The first formed product

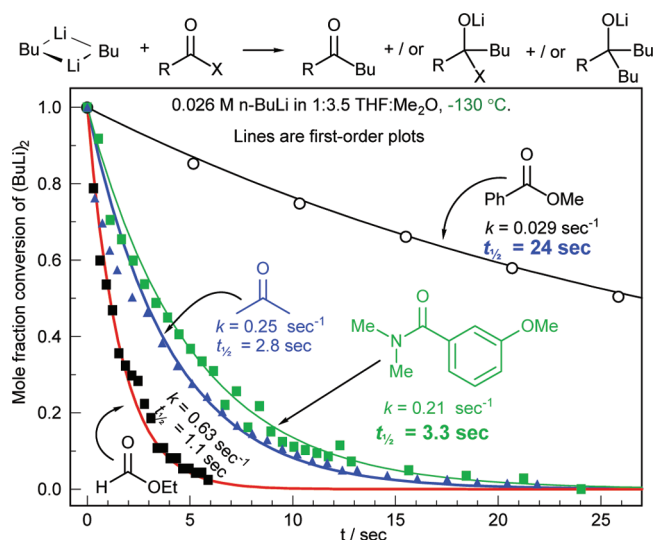


Figure 25. Kinetic experiments on the rate of reaction of  $(\text{BuLi})_2$  with several carbonyl compounds.<sup>36e</sup>

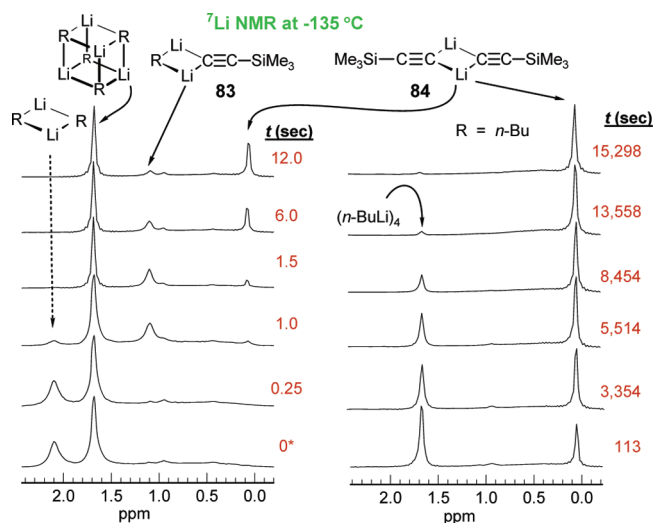


Figure 26. Sample RINMR experiment followed by  $^7\text{Li}$  NMR spectroscopy: reaction of *n*-BuLi dimer and tetramer with trimethylsilylacetylene at  $-130\text{ }^{\circ}\text{C}$  in 3:1  $\text{Me}_2\text{O}/\text{THF}$ .<sup>50</sup>

is a mixed dimer **83**, which reacts more slowly with the acetylene (by a factor of 42) to form the lithium acetylide homodimer **84**. The *n*-BuLi tetramer reacts over a period of several hours, but this process is zero order in acetylene and corresponds to the rate of tetramer dissociation ( $k = 0.0002\text{ s}^{-1}$ ). These data show that the dimer is at least 40000 times as reactive as tetramer. However, this is an underestimate at both ends, since reaction of the dimer is too fast to be measured and the tetramer does not react.

Our strategy for obtaining an actual rate comparison was to study progressively more acidic acetylenes until one was found which reacted with the *n*-BuLi tetramer. Trimethylsilylacetylene reacted a little too quickly for our apparatus, but the deuterated isotopomer was comfortably in range ( $k = 2.2\text{ M}^{-1}\text{ s}^{-1}$  at  $-130\text{ }^{\circ}\text{C}$ ). After measurement of the isotope effect ( $k_{\text{H}}/k_{\text{D}} = 52$ ), we could calculate the rate of the protio analogue ( $k = 114\text{ M}^{-1}\text{ s}^{-1}$ ).  $\text{Ph}_3\text{Si}-\text{C}\equiv\text{C}-\text{H}$  was 66 times faster and  $\text{PhS}-\text{C}\equiv\text{C}-\text{H}$  3800 times faster than  $\text{Me}_3\text{Si}-\text{C}\equiv\text{C}-\text{H}$ , as measured by competition experiments. The latter did react with the tetramer



just a little faster than tetramer dissociated. From the extrapolated rate of the dimer and measured rate of the tetramer we calculate that *n*-BuLi dimer is 320,000,000 times as reactive as the tetramer toward PhS–C≡C–H at –130 °C, an unprecedentedly large number for such a comparison.

We also studied the reaction of several aldehydes with *n*-BuLi. Their behavior is complicated and not completely understood. Both benzaldehyde and *p*-(dimethylamino)-benzaldehyde reacted with the dimer in less than 1 s at –135 °C. Benzaldehyde reacted slowly with the tetramer (competitive with dissociation) whereas the *p*-(dimethylamino)-benzaldehyde did not. Thus, here also the dimer is much more reactive than the tetramer, by factors of at least 5800 and 18000. In his pioneering work, McGarrity had estimated that this rate ratio was ca. 10 at –86 °C, a number that must be a serious underestimate due to the narrow dynamic range at the temperature used.<sup>69a</sup> This was the only measured value available for such a comparison until our experiments were reported.

One of the surprising effects we observed is the remarkably small reactivity differences shown by various reactions of the BuLi dimer, considering that such differences are expected to be considerably magnified at very low temperatures. We have already mentioned the ketone/ester/amide experiments (Figure 25) which cover a total range of only a factor of 10. The difference in the rate of reaction of *m*-F and *p*-F *N,N*-dimethylbenzamide with (BuLi)<sub>2</sub> was 1:1.03 and for the methyl benzoates, 1.4.<sup>36f</sup> For comparison, the rates of aldol reactions of *p*-fluoroacetophenone with *m*-F and *p*-F benzaldehyde differ by a factor of 4.7.<sup>43c</sup> This speaks to a very close balance between electrophilic and nucleophilic activation in BuLi reactions, and to the development of little charge at the transition state. Compare some of these rate ratios to the huge numbers found for the reactions of **42** discussed below, which are clearly much more ionic in nature.

**Take-Home Lesson.** For synthetic chemists using *n*-BuLi it is worthwhile to note that for many of the common reactions in THF the rate determining step is dissociation of the tetramer/hexamer mixture in the commercial hexane solution to the active dimers, and that this process is over in under 10 ms at –78 °C. So hour-long reaction times followed by warming to 0 °C to “finish” the reaction (as one often finds in experimental descriptions) are, to put it mildly, overkill and may well allow initially pristine solutions to decay.

## RINMR STUDIES OF TRIS(TRIMETHYLSILYL)METHYLLITHIUM

We actually constructed our RINMR apparatus specifically for performing experiments on the unique (Me<sub>3</sub>Si)<sub>3</sub>CLi system **42**. Solutions of **42** contain nearly equal quantities of three species, the triple ion (TI), SIP, and CIP, species which are surely of great importance for organolithium mechanisms in general. Two of the key spectra of <sup>13</sup>C and <sup>6</sup>Li enriched material used to characterize **42** are shown in Figure 27. The three species had exceptionally high barriers to interconversion (the entire gray-black region in Figure 24) and thus looked like a rich system for study,<sup>34e,51,52</sup> albeit in a structure with unusually high steric demands and hence hardly a typical lithium reagent.<sup>71</sup>

Reactions of **42** with methyl iodide were straightforward; the SIP reacted too fast for us to measure at –130 °C (half-life under 1 s), and neither the CIP nor the TI reacted directly (zero order in MeI). In each case, the rate-limiting step was dissociation of the species to the SIP. We could show that the

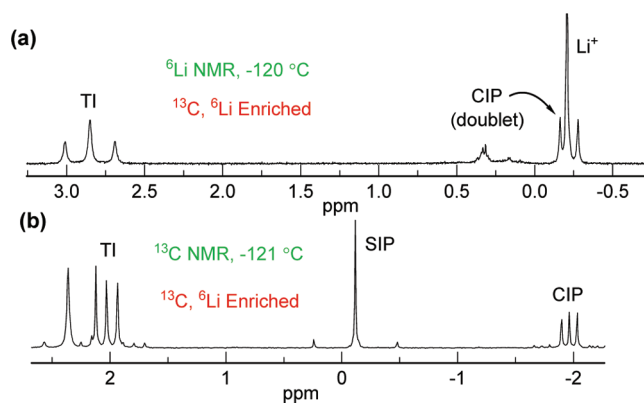


**Figure 27.** Part of the structure proof for the unusual species present in solutions of doubly enriched **42**: (a) <sup>6</sup>Li and (b) <sup>13</sup>C spectra of C–Li carbon in 3:2 THF/ether. The triplet in the <sup>6</sup>Li NMR spectrum at δ 2.7 corresponds to Li bonded to two carbons of **42**-TI, the carbon 1:1:1 triplet at δ 2.0 to a carbon bonded to one lithium.

SIP is >100 times as reactive as the CIP and >10<sup>9</sup> as reactive as the TI. True numbers are larger (for the CIP probably *very much* larger), but we were at the limits of available dynamic range.<sup>52</sup>

Benzaldehydes also did not react with **42**-CIP, which dissociates faster than it reacts. Reactions of **42**-TI are more complicated. Although a reaction first order in aldehyde was seen, it turned out not to be an addition reaction, but an aldehyde catalyzed dissociation of the TI to the more reactive SIP, which then reacts in a separate step. This explains why electron-rich aldehydes react much more rapidly than electron-deficient ones, and the curious observation that the order of reactivity is reversed when competition experiments between aldehydes were performed. The more electron-rich (less reactive) aldehydes were more active in dissociating the TI, but in the subsequent competition for the SIP/CIP, the electron-deficient aldehydes won (Figure 28).<sup>52</sup>

These experiments provided several interesting rate comparisons. The SIP is at least 10<sup>9</sup> as reactive as the TI toward 3,5-bistrifluoromethylbenzaldehyde at –130 °C. The addition of excess HMPA reduced the rate of addition of the SIP to *p*-(diethylamino)benzaldehyde by >10<sup>10</sup> at –130 °C. Thus, the

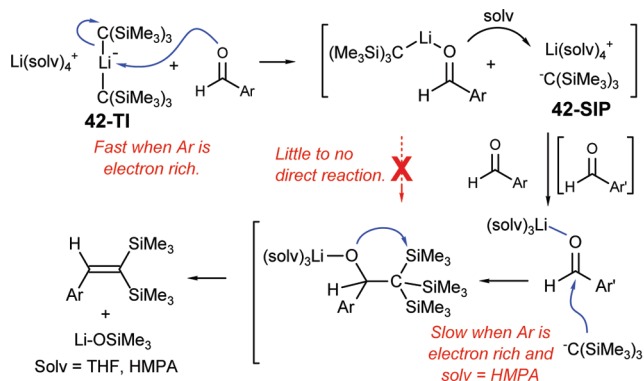


**Figure 28.** Mechanistic path for reaction of benzaldehydes with **42**-TI. When two different aldehydes are present, the electron-rich one cleaves the triple ion, but the electron-poor one reacts preferentially with the monomeric lithium species, leading to inverse rate and selectivity effects.<sup>52</sup>

lithium ion accelerating effect, partially or completely destroyed by HMPA, is at least this large.

The alert student (Bill Sikorski) who did much of the NMR work with **42** noticed that the CH  $^{13}\text{C}$  NMR shift of the small amount of  $(\text{Me}_3\text{Si})_3\text{CH}$  present in most of the samples moved around quite dramatically as sample temperature was changed. He developed this into a very effective  $^{13}\text{C}$  NMR chemical shift thermometer, which permits accurate, easy, and efficient measurement of the true sample temperature during variable-temperature NMR experiments (Figure 29). We have employed it in virtually all low-temperature NMR experiments during the last 15 years.<sup>34e,77</sup>

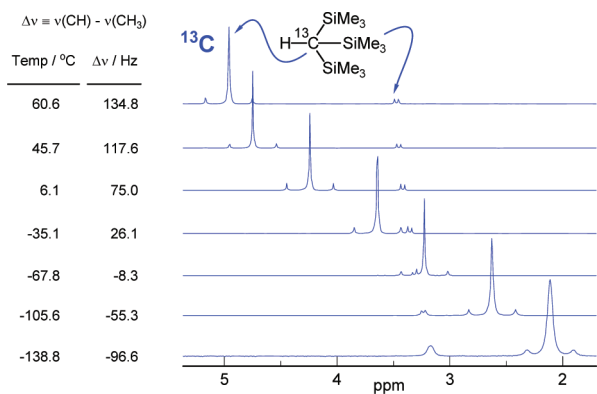


**Figure 29.** Temperature dependence of the  $^{13}\text{C}$  chemical shifts of the CH (100%  $^{13}\text{C}$  enriched) and  $\text{SiCH}_3$  signals.<sup>77</sup> The nearly linear dependence of the difference in the two chemical shifts allows accurate in situ measurements of sample temperature.

## RINMR STUDIES OF ENOLATE FORMATION AND REACTIVITY

One of the best known, much studied, and often used reactions of enolates is the aldol reaction. Amazingly, there have been almost no direct kinetic studies of the lithium enolate aldol process.<sup>70</sup> There is a reason for this: the reaction is simply too fast. We have applied the RINMR apparatus for the first detailed kinetic study of several aldol processes, most notably those of *p*-fluoroacetophenone enolate with fluorobenzaldehydes. The  $^{19}\text{F}$  labels were crucial for successful RINMR experiments.<sup>43c</sup>

**Enolate Formation.** We started with an examination of the formation of the lithium enolate by deprotonation of ketone with LDA, a process that has also been outside the range of normal kinetic studies. The reaction of LDA dimer in THF at  $-125^\circ\text{C}$  with *p*-fluoroacetophenone led first to a mixed LDA–enolate dimer **85**, which continued a little more slowly to the enolate dimer. Note that the stable aggregate structure of this enolate in THF is exclusively tetrameric, so this dimer is a metastable species. It has a long enough lifetime that a variety of studies can be performed on it, even though it is present in vanishingly small concentrations at equilibrium ( $K_{\text{eq}} = \text{T}/\text{D}^2 \geq 1.3 \times 10^6 \text{ M}^{-1}$  at  $-120^\circ\text{C}$ ). In a much slower second-order process (half-life of several hours), the dimer then dimerizes to the tetramer (Figure 30). This behavior provided an almost unprecedented opportunity in organolithium chemistry to independently study essentially pure solutions of two different aggregates of a lithium reagent under identical conditions.

Remarkably, even a metastable monomeric complex of *p*-fluoroacetophenone enolate (**86**) can be prepared if the

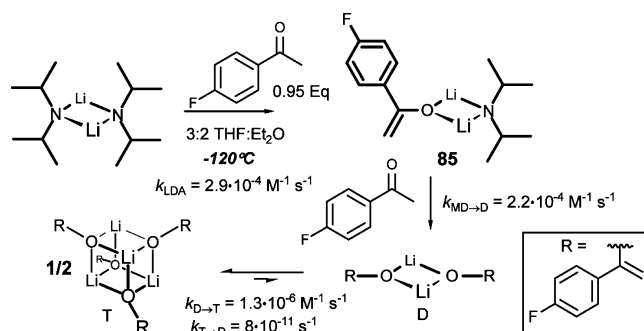
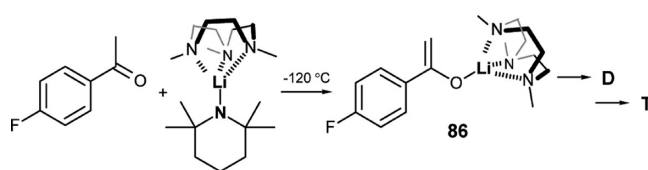


**Figure 30.** Kinetic scheme for the deprotonation of *p*-fluoroacetophenone with LDA dimer.<sup>43c</sup>

deprotonation is performed with a monomeric amide base, the TMTAN complex of lithium tetramethylpiperidine.<sup>2h</sup> The monomeric enolate has a half-life of 40 min at  $-120^\circ\text{C}$  for loss of TMTAN and conversion to the dimer and then to the stable tetramer.



**Aldol Reaction.** A detailed kinetic study of the aldol reaction of acetophenone enolate tetramer showed some interesting behavior. The reaction was first order in tetramer and aldehyde, forming just one detectable intermediate, a 3:1 enolate–aldolate mixed tetramer **87**.<sup>56e</sup> This mixed tetramer was itself kinetically active and 2–3 times as reactive as the homotetramer, so it never built up to more than 25% of the reaction mixture (Figure 31). All subsequent steps in the aldol process are fast. Either the higher mixed tetramers are still more reactive, or they dissociate to more reactive dimers. A brief Hammett study of substituted aldehydes showed the expected

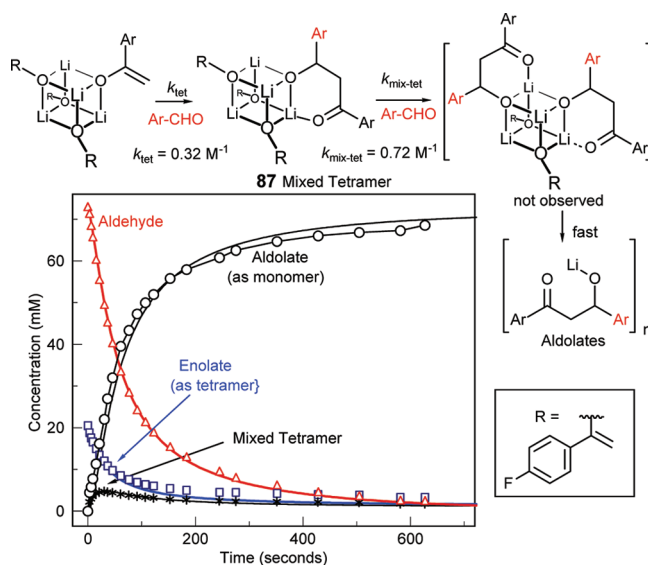


**Figure 31.** Kinetics of a tetrameric enolate aldol reaction at  $-125^\circ\text{C}$  in 3:2 THF/ether. The lines are simulations using the two rate constants shown.<sup>43c</sup>

response, with electron deficient aldehydes being more reactive than electron rich ones ( $\rho = 4.0$ ).

Direct comparison of the enolate dimer and tetramer aldol reactions could either be done by individual kinetic runs, or on a 1:1 mixture of the two aggregates produced by forming the dimer in a RINMR experiment, allowing the tetramerization to proceed halfway and then injecting benzaldehyde. Both techniques showed the dimer to react about 20x as fast as tetramer. Both aldol reactions were faster than interconversion of the dimer and tetramer enolates. This small difference is in sharp contrast to our previous aggregate comparisons for *n*-BuLi dimer and tetramer, which gave much larger numbers. The Streitwieser group has also measured several aggregate relative reactivities and also found relatively small values.<sup>5</sup>

## ■ CLOSING THOUGHTS

Multinuclear NMR studies at the lowest possible temperatures can provide detailed information about the species present in organolithium solutions and can define the energetics of their interconversion. When combined with an efficient and rugged mixing device, RINMR kinetic studies become possible which in favorable cases can operate under non-Curtin–Hammett conditions, providing exceptionally clear insights into some of the molecular processes involved in organolithium reactions.

At the beginning of this article, I pointed to the sparse knowledge of the behavior of organolithium aggregates and mixed aggregates. This situation is being actively remedied by studies in several laboratories, but we are certainly not in a position to make broad generalizations. The long accepted one that higher aggregates are less reactive has held up well to closer scrutiny, but the actual reactivity differences, and particularly their chemical consequences are still largely unknown. We have provided several examples of nonaggregated lithium reagents in which the interplay between contact and separated ion pairs controls the reactivity.

Mixed aggregates have been frequently detected, but these have almost always been equilibrium situations under Curtin–Hammett control. Although it is entirely rational that when an organolithium aggregate reacts with a substrate the first-formed product is a mixed aggregate at the same stage of aggregation, this had not been directly demonstrated. In the work described above, and in other unpublished work direct formation of mixed aggregates under non-Curtin–Hammett conditions has been detected, including some where the mixed aggregates had significantly different chemistry than the homoaggregate precursors.

The research described here has been greatly facilitated by a computer program I wrote (WINDNMR) which allows the simulation of a variety of NMR spectra, including DNMR spectra for kinetic measurements using full line shape analysis. I have made this program freely available to the general user.<sup>78a</sup> There is a companion program (WINPLT) which allows the graphical presentation of chemical structures, NMR spectra, graphs and other material. All of the graphics in this paper were prepared with this program,<sup>78b</sup> as were several websites that many chemists have found useful, including the Bordwell  $pK_a$  site<sup>79a</sup> and the total synthesis site.<sup>79b</sup>

## ■ AUTHOR INFORMATION

### Corresponding Author

\*Email: reich@chem.wisc.edu.

## Notes

The authors declare no competing financial interest.

## Biography



Hans J. Reich was born in Germany, emigrated to Canada as a child, and received his B.Sc. at the University of Alberta. After his Ph.D. work at UCLA in the Cram group and postdoctoral studies with Roberts at CalTech and Woodward at Harvard, he started his independent career at the University of Wisconsin, Madison in 1970. His research program has included synthetic and mechanistic studies involving organic compounds of selenium, silicon, tin, sulfur, tellurium, lithium, and others.

## ■ ACKNOWLEDGMENTS

I am grateful to the National Science Foundation for their generous support over the decades, mostly in the Synthetic Organic and Natural Products Chemistry Program. The work summarized here resulted from the measurement of tens of thousands of nonroutine NMR spectra. The vast majority of these were measured at temperatures well below  $-100\text{ }^\circ\text{C}$ , with all the attendant problems of icing, freezing, crystallization, temperature measurement, and inexplicable line broadening. The frequency with which we could say, while analyzing such spectra, that we have discovered a species, measured an effect, or seen a phenomenon never before seen has been very satisfying. This has certainly helped the many very capable and dedicated graduate students, several postdocs, and a number of undergraduate researchers involved keep up their intensity through those many other experiments which could only be characterized as boring (although necessary), not to mention the dismaying number of unsuccessful ones. I am grateful to all for their hard work, intellectual contributions, perseverance, and sometimes heroic efforts to solve the structural and kinetic puzzles we encountered.

## ■ REFERENCES

- (1) Gossage, R. A.; Jastrzebski, J. T. B. H.; van Koten, G. *Angew. Chem., Int. Ed. Engl.* **2005**, *44*, 1448–1454.
- (2) (a) Briggs, T. F.; Winemiller, M. D.; Collum, D. B.; Parsons, R. L., Jr.; Davulcu, A. H.; Harris, G. D.; Fortunak, J. M.; Confalone, P. N. *J. Am. Chem. Soc.* **2004**, *126*, 5427–5435. Singh, K. J.; Collum, D. B. *J. Am. Chem. Soc.* **2006**, *128*, 13753–13760. Riggs, J. C.; Singh, K. J.; Yun, M.; Collum, D. B. *J. Am. Chem. Soc.* **2008**, *130*, 13709–13717. (b) Romesberg, F. E.; Gilchrist, J. H.; Harrison, A. T.; Fuller, D. J.; Collum, D. B. *J. Am. Chem. Soc.* **1991**, *113*, 5751–5757. Romesberg, F. E.; Bernstein, M. P.; Gilchrist, J. H.; Harrison, A. T.; Fuller, D. J.; Collum, D. B. *J. Am. Chem. Soc.* **1993**, *115*, 3475–3483. (c) Liou, L. R.; McNeil, A. J.; Ramirez, A.; Toombes, G. E. S.; Gruver, J. M.;

- Collum, D. B. *J. Am. Chem. Soc.* **2008**, *130*, 4859–4868. (d) Ramirez, A.; Candler, J.; Bashore, C. G.; Wirtz, M. C.; Coe, J. W.; Collum, D. B. *J. Am. Chem. Soc.* **2004**, *126*, 14700–14701. (e) Hoepker, A. C.; Gupta, L.; Ma, Y.; Faggini, M. F.; Collum, D. B. *J. Am. Chem. Soc.* **2011**, *133*, 7135–7151. (f) Qu, B.; Collum, D. B. *J. Am. Chem. Soc.* **2005**, *127*, 10820–10821. (g) Chadwick, S. T.; Rennels, R. A.; Rutherford, J. L.; Collum, D. B. *J. Am. Chem. Soc.* **2000**, *122*, 8640–8647. (h) Remenar, J. F.; Lucht, B. L.; Kruglyak, D.; Romesberg, F. E.; Gilchrist, J. H.; Collum, D. B. *J. Org. Chem.* **1997**, *62*, 5748–5754.
- (3) (a) Sott, R.; Granander, J.; Hilmersson, G. *J. Am. Chem. Soc.* **2004**, *126*, 6798–6805.
- (4) Jackman, L. M.; Lange, B. C. *J. Am. Chem. Soc.* **1981**, *103*, 4494–4499.
- (5) (a) Abu-Hasanayn, F.; Streitwieser, A. *J. Am. Chem. Soc.* **1996**, *118*, 8136–8137. (b) Streitwieser, A.; Leung, S. S.-W.; Kim, Y.-J. *Org. Lett.* **1999**, *1*, 145–147.
- (6) Sugawara, K.; Shindo, M.; Noguchi, H.; Koga, K. *Tetrahedron Lett.* **1996**, *37*, 7377–7380. Lecachey, B.; Duguet, N.; Oulyadi, H.; Fressign, C.; Harrison-Marchand, A.; Yamamoto, Y.; Tomioka, K.; Maddaluno, J. *Org. Lett.* **2009**, *11*, 1907–1910. Pratt, L. M.; Newman, A.; St. Cyr, J.; Johnson, H.; Miles, B.; Lattier, A.; Austin, E.; Henderson, S.; Hershey, B.; Lin, M.; Balamraju, Y.; Sammonds, L.; Cheramie, J.; Karnes, J.; Hymel, E.; Woodford, B.; Carter, C. *J. Org. Chem.* **2003**, *68*, 6387. Liu, J.; Li, D.; Sun, C.; Williard, P. G. *J. Org. Chem.* **2008**, *73*, 4045–4052.
- (7)  $\alpha$ -Lithio selenoxides: Reich, H. J.; Shah, S. K. *J. Am. Chem. Soc.* **1975**, *97*, 3250. Reich, H. J.; Shah, S. K.; Chow, F. *J. Am. Chem. Soc.* **1979**, *101*, 6648–6656.
- (8) Lithiated allyl and vinyl selenides: (a) Reich, H. J. *J. Org. Chem.* **1975**, *40*, 2570. Reich, H. J.; Clark, M. C.; Willis, W. W., Jr. *J. Org. Chem.* **1982**, *47*, 1618–6623. (b) Reich, H. J.; Willis, W. W., Jr. *J. Org. Chem.* **1980**, *45*, 5227. (c) Reich, H. J.; Willis, W. W., Jr. *J. Org. Chem.* **1980**, *45*, 5227.
- (9) Lithiated propargyl selenides: (a) Reich, H. J.; Shah, S. K. *J. Am. Chem. Soc.* **1977**, *99*, 263–265. Reich, H. J.; Gold, P. M.; Chow, F. *Tetrahedron Lett.* **1979**, 4433–4434. (b) Reich, H. J.; Shah, S. K.; Gold, P. M.; Olson, R. E. *J. Am. Chem. Soc.* **1981**, *103*, 3112–3120.
- (10) Reich, H. J.; Shah, S. K. *J. Org. Chem.* **1977**, *42*, 1773. Reich, H. J.; Cohen, M. L. *J. Am. Chem. Soc.* **1979**, *101*, 1307. Reich, H. J.; Chow, F.; Shah, S. K. *J. Am. Chem. Soc.* **1979**, *101*, 6638–6648.
- (11) Reich, H. J.; Bowe, M. D. *J. Am. Chem. Soc.* **1990**, *112*, 8994–8995.
- (12) (a) Reich, H. J.; Dykstra, R. R. *Angew. Chem., Int. Ed. Engl.* **1993**, *32*, 1469–1470. (b) Reich, H. J.; Dykstra, R. R. *J. Am. Chem. Soc.* **1993**, *115*, 7041–7042.
- (13) Reich, H. J.; Rusek, J. J.; Olson, R. E. *J. Am. Chem. Soc.* **1979**, *101*, 2225–2227.
- (14) (a) Brook, A. G. *Acc. Chem. Res.* **1974**, *1*, 77–84. (b) Moser, W. H. *Tetrahedron* **2001**, *57*, 2065–2084.
- (15) (a) Reich, H. J.; Kelly, M. J.; Olson, R. E.; Holtan, R. C. *Tetrahedron* **1983**, *39*, 949. (b) Reich, H. J.; Kelly, M. J. *J. Am. Chem. Soc.* **1982**, *104*, 1119. Reich, H. J.; Holtan, R. C.; Borkowsky, S. I. *J. Org. Chem.* **1987**, *52*, 312. Reich, H. J.; Holtan, R. C.; Bolm, C. *J. Am. Chem. Soc.* **1990**, *112*, 5609–5617.
- (16) (a) Corey, E. J.; Luo, G.; Lin, L. S. *J. Am. Chem. Soc.* **1997**, *119*, 9927–9928. (b) Mi, Y.; Schreiber, J. V.; Corey, E. J. *J. Am. Chem. Soc.* **2002**, *124*, 11290–11291.
- (17) (a) Reich, H. J.; Olson, R. E.; Clark, M. C. *J. Am. Chem. Soc.* **1980**, *102*, 1423. (b) Reich, H. J.; Eisenhart, E. K.; Olson, R. E.; Kelly, M. J. *J. Am. Chem. Soc.* **1986**, *108*, 7791–7800.
- (18) We were not the only ones to develop this concept: Kuwajima, I.; Kato, M. *Chem. Commun.* **1979**, 708.
- (19) We did not address this question but did initiate a major investigation of other main-group ate complexes (see later sections). We were able to rule out siliconates as reactive intermediates in several Sakurai reactions: Biddle, M. M.; Reich, H. J. *J. Org. Chem.* **2006**, *71*, 4031–4039.
- (20) (a) Fraenkel, G.; Geckle, J. M. *J. Am. Chem. Soc.* **1980**, *102*, 2869. (b) Fraenkel, G.; Halasa, A. F.; Mochel, V.; Stumpe, R.; Tate, D. *J. Org. Chem.* **1985**, *50*, 4563–4565. (c) Fraenkel, G.; Winchester, W. R. *J. Am. Chem. Soc.* **1988**, *110*, 8720–8721.
- (21) Ando, K.; Takemasa, Y.; Tomioka, K.; Koga, K. *Tetrahedron* **1993**, *49*, 1579–1588.
- (22) Little, R. D.; Dawson, J. R. *J. Am. Chem. Soc.* **1978**, *100*, 4607.
- (23) Coe, J. W.; Wirtz, M. C.; Bashore, C. G.; Candler, J. *Org. Lett.* **2004**, *6*, 1589–1592.
- (24) (a) Winchester, W. R.; Bauer, W.; Schleyer, P. v. R. *J. Chem. Soc., Chem. Commun.* **1987**, 177–179. (b) Bauer, W.; Winchester, W. R.; Schleyer, P. v. R. *Organometallics* **1987**, *6*, 2371–2379. (c) Lambert, C.; Schleyer, P. v. R.; Würthwein, E.-U. *J. Org. Chem.* **1993**, *58*, 6377–6389.
- (25) Biellmann, J. F.; Ducep, J. B. *Org. React.* **1982**, *27*, 1.
- (26) (a) Reich, H. J.; Holladay, J. E.; Mason, J. D.; Sikorski, W. H. *J. Am. Chem. Soc.* **1995**, *117*, 12137–12150. (b) Reich, H. J.; Mason, J. D.; Holladay, J. E. *J. Chem. Soc., Chem. Commun.* **1993**, 1481–1483.
- (27) Allenyllithium reagents: (a) Reich, H. J.; Reich, I. L.; Yelm, K. E.; Holladay, J. E.; Gschneidner, D. *J. Am. Chem. Soc.* **1993**, *115*, 6625–6635. (b) Reich, H. J.; Holladay, J. E. *J. Am. Chem. Soc.* **1995**, *117*, 8470–8471. (c) Reich, H. J.; Holladay, J. E. *Angew. Chem. Int. Ed., Engl.* **1996**, *35*, 2365–2367. (d) Reich, H. J.; Holladay, J. E.; Walker, T. G.; Thompson, J. L. *J. Am. Chem. Soc.* **1999**, *121*, 9769–9780. (e) Reich, H. J.; Thompson, J. L. *Org. Lett.* **2000**, *2*, 783–786.
- (28) Lithium–tin exchange: (a) Reich, H. J.; Phillips, N. H. *J. Am. Chem. Soc.* **1986**, *108*, 2102–2103. (b) Reich, H. J.; Phillips, N. H. *Pure Appl. Chem.* **1987**, *59*, 1021–1026. (c) Reich, H. J.; Borst, J. P.; Coplien, M. B.; Phillips, N. H. *J. Am. Chem. Soc.* **1992**, *114*, 6577–6579.
- (29) Hoppe, D.; Riemenschneider, C. *Angew. Chem., Int. Ed. Engl.* **1983**, *22*, 54.
- (30) Chelation in aryllithium reagents: (a) Reich, H. J.; Kulicke, K. J. *J. Am. Chem. Soc.* **1995**, *117*, 6621–6622. (b) Reich, H. J.; Kulicke, K. J. *J. Am. Chem. Soc.* **1996**, *118*, 273–274. (c) Reich, H. J.; Gudmundsson, B. Ö. *J. Am. Chem. Soc.* **1996**, *118*, 6074–6075. Reich, H. J.; Goldenberg, W. S.; Gudmundsson, B. Ö.; Sanders, A. W.; Kulicke, K. J.; Simon, K.; Guzei, I. A. *J. Am. Chem. Soc.* **2001**, *123*, 8067–8079. (d) Reich, H. J.; Goldenberg, W. S.; Sanders, A. W.; Jantzi, K. L.; Tzschucke, C. C. *J. Am. Chem. Soc.* **2003**, *125*, 3509–3521. Reich, H. J.; Goldenberg, W. S.; Sanders, A. W.; Tzschucke, C. C. *Org. Lett.* **2001**, *3*, 33–36. (e) Jantzi, K. L.; Puckett, C. L.; Guzei, I. L.; Reich, H. J. *J. Org. Chem.* **2005**, *70*, 7520–7529. (f) Jantzi, K. L.; Guzei, I. L.; Reich, H. J. *Organometallics* **2006**, *25*, 5390–5395. (g) Reich, H. J.; Goldenberg, W. S.; Sanders, A. W. *ARKIVOC* **2004**, (xiii), 97–129, [http://www.arkat-usa.org/ark/journal/2004/I13\\_Krohn/1230/KK-1230F.asp](http://www.arkat-usa.org/ark/journal/2004/I13_Krohn/1230/KK-1230F.asp).
- (31) Reich, I. L.; Reich, H. J. *J. Org. Chem.* **1981**, *46*, 3721–3727. Reich, I. L.; Reich, H. J. *J. Org. Chem.* **1990**, *55*, 2282–2283.
- (32) Reich, H. J.; Yelm, K. E.; Reich, I. L. *J. Org. Chem.* **1984**, *49*, 3438–3440.
- (33) Wittig, G.; Schollkopf, U. *Tetrahedron* **1958**, *3*, 91–93.
- (34) Lithium–iodine exchange: (a) Reich, H. J.; Phillips, N. H.; Reich, I. L. *J. Am. Chem. Soc.* **1985**, *107*, 4101–4103. (b) Reich, H. J.; Green, D. P.; Phillips, N. H. *J. Am. Chem. Soc.* **1989**, *111*, 3444–3445. (c) Reich, H. J.; Green, D. P.; Phillips, N. H. *J. Am. Chem. Soc.* **1991**, *113*, 1414–1416. (d) Reich, H. J.; Whipple, W. L. *Can. J. Chem.* **2005**, *83*, 1577–1587. (e) Reich, H. J.; Sikorski, W. H.; Sanders, A. W.; Jones, A. C.; Plessel, K. N. *J. Org. Chem.* **2009**, *74*, 719–729. (f) Reich, H. J.; Green, D. P.; Phillips, N. H.; Borst, J. P.; Reich, I. L. *Phosphorus Sulfur* **1992**, *67*, 83–97.
- (35) Lithium–tellurium and lithium–selenium exchange: (a) Reich, H. J.; Gudmundsson, B. Ö.; Green, D. P.; Bevan, M. J.; Reich, I. L. *Helv. Chim. Acta* **2002**, *85*, 3748–3772. (b) Reich, H. J.; Bevan, M. J.; Gudmundsson, B. Ö.; Puckett, C. L. *Angew. Chem., Int. Ed.* **2002**, *41*, 3436–3439. (c) Reich, H. J.; Gudmundsson, B. Ö.; Dykstra, R. R. *J. Am. Chem. Soc.* **1992**, *114*, 7937–7938.
- (36) (a) Bevan, M. J. Ph.D. Thesis, University of Wisconsin, Madison, 2003. (b) Sikorski, W. H. Ph.D. Thesis, University of Wisconsin, Madison, 1997. (c) Thompson, J. L. Ph.D. Thesis, University of Wisconsin, Madison, 1999. (d) Smith, K. A. MS Thesis,

University of Wisconsin, Madison, 2005. (e) Jones, A. C. Ph.D. Thesis, University of Wisconsin, Madison, 2007. (f) Plessel, K. N. Ph.D. Thesis, University of Wisconsin, Madison, 2008.

(37) de Keijzer, A. H. J. F.; de Kanter, F. J. J.; Schakel, M.; Schmitz, R. F.; Klumpp, G. W. *Angew. Chem., Int. Ed. Engl.* **1996**, *35*, 1127–1128.

(38) Boche, G.; Schimeczek, M.; Cioslowski, J.; Piskorz, P. *Eur. J. Org. Chem.* **1998**, 1851–1860.

(39) Kanda, T.; Kato, S.; Kambe, N.; Kohara, Y.; Sonoda, N. *J. Phys. Org. Chem.* **1996**, *9*, 29–34.

(40) Enone addition regioselectivity: (a) Sikorski, W. H.; Reich, H. J. *J. Am. Chem. Soc.* **2001**, *123*, 6527–6535. (b) Reich, H. J.; Sikorski, W. H. *J. Org. Chem.* **1999**, *64*, 14–15.

(41) HMPA titration method: (a) Reich, H. J.; Borst, J. P. *J. Am. Chem. Soc.* **1991**, *113*, 1835–1837. (b) Reich, H. J.; Borst, J. P.; Dykstra, R. R.; Green, D. P. *J. Am. Chem. Soc.* **1993**, *115*, 8728–8741. (c) Reich, H. J.; Borst, J. P.; Dykstra, R. R. *Organometallics* **1994**, *13*, 1–3. (d) Reich, H. J.; Borst, J. P.; Dykstra, R. R. *Tetrahedron* **1994**, *50*, 5869–5880.

(42) Reich, H. J.; Green, D. P.; Medina, M. A.; Goldenberg, W. S.; Gudmundsson, B. Ö.; Dykstra, R. R.; Phillips, N. H. *J. Am. Chem. Soc.* **1998**, *120*, 7201–7210.

(43) Enolate structure and dynamics: (a) Kolonko, K. J.; Biddle, M. M.; Guzei, I. A.; Reich, H. J. *J. Am. Chem. Soc.* **2009**, *131*, 11525–11534. (b) Kolonko, K. J.; Guzei, I. A.; Reich, H. J. *J. Org. Chem.* **2010**, *75*, 6163–6172. (c) Kolonko, K. J.; Wherritt, D. J.; Reich, H. J. *J. Am. Chem. Soc.* **2011**, *133*, 16774–16777. (d) Kolonko, K. J.; Reich, H. J. *J. Am. Chem. Soc.* **2008**, *130*, 9668–9669.

(44) Carlier, P. R.; Lo, C. W.-S. *J. Am. Chem. Soc.* **2000**, *122*, 12819–12823.

(45) Denmark, S. E.; Swiss, K. A. *J. Am. Chem. Soc.* **1993**, *115*, 12195–12196.

(46) Jackman, L. M.; Chen, X. *J. Am. Chem. Soc.* **1992**, *114*, 403–411.

(47) Reich, H. J.; Sikorski, W. H.; Gudmundsson, B. Ö.; Dykstra, R. R. *J. Am. Chem. Soc.* **1998**, *120*, 4035–4036.

(48) Such a complex for LiBr was characterized both by NMR spectroscopy and by single-crystal X-Ray. Barr, D.; Doyle, M. J.; Mulvey, R. E.; Raithby, P. R.; Reed, D.; Snaith, R.; Wright, D. S. *J. Chem. Soc., Chem. Commun.* **1989**, 318.

(49) Eaborn, C.; Hitchcock, P. B.; Smith, J. D.; Sullivan, A. C. *J. Chem. Soc., Chem. Commun.* **1983**, 827–828.

(50) Jones, A. C.; Sanders, A. W.; Bevan, M. J.; Reich, H. J. *J. Am. Chem. Soc.* **2007**, *129*, 3492–3493.

(51) Reich, H. J.; Sikorski, W. H.; Thompson, J. L.; Sanders, A. W.; Jones, A. C. *Org. Lett.* **2006**, *8*, 4003–4006.

(52) Jones, A. C.; Sanders, A. W.; Sikorski, W. H.; Jansen, K. L.; Reich, H. J. *J. Am. Chem. Soc.* **2008**, *130*, 6060–6061.

(53) Jones, F. N.; Zinn, M. F.; Hauser, C. R. *J. Org. Chem.* **1963**, *28*, 663–665.

(54) (a) Pearson, W. H.; Lindbeck, A. C. *J. Am. Chem. Soc.* **1991**, *113*, 8546–48. (b) Gawley, R. E.; Zhang, Q. *J. Am. Chem. Soc.* **1993**, *115*, 7515–6. (c) Kerrick, S. T.; Beak, P. *J. Am. Chem. Soc.* **1991**, *113*, 9708–10. Chong, J. M.; Park, S. B. *J. Org. Chem.* **1992**, *57*, 2220–2222. Stead, D.; Carbone, G.; O'Brien, P.; Campos, K. R.; Coldham, I.; Sanderson, A. *J. Am. Chem. Soc.* **2010**, *132*, 7260–7261.

(55) Rotation controlled enantiomerization was also observed for other related systems: Ahlbrecht, H.; Harbach, J.; Hoffmann, R. W.; Ruhland, T. *Lieb. Ann.* **1995**, 211–216.

(56) (a) Seebach, D.; Peleties, N. *Chem. Ber.* **1972**, *105*, 511–520. (b) Seebach, D.; Beck, A. K. *Chem. Ber.* **1975**, *108*, 314. (c) Juaristi, E.; Hernandez-Rodriguez, M.; Lopez-Ruis, H.; Avina, J.; Munoz-Muniz, O.; Hayakawa, M.; Seebach, D. *Helv. Chim. Acta* **2002**, *85*, 1999–2008. (d) Heinzer, J.; Oth, J. F. M.; Seebach, D. *Helv. Chim. Acta* **1985**, *68*, 1848–1862. (e) Seebach, D.; Amstutz, R.; Dunitz, J. D. *Helv. Chim. Acta* **1981**, *64*, 2622–2626.

(57) Reich, H. J.; Medina, M. A.; Bowe, M. D. *J. Am. Chem. Soc.* **1992**, *114*, 11003–11004.

(58) Tomoki, H.; Kambe, N.; Ogawa, A.; Miyoshi, N.; Murai, S.; Sonoda, N. *Angew. Chem., Int. Ed. Engl.* **1987**, *26*, 1187.

(59) (a) Cram, D. J.; Wong, S. M. C.; Fischer, H. P. *J. Am. Chem. Soc.* **1971**, *93*, 2235–2243. (b) Cram, D. J.; Gosser, L. *J. Am. Chem. Soc.* **1964**, *86*, 5457–5465.

(60) Brown, C. A.; Yamaichi, A. *J. Chem. Soc., Chem. Commun.* **1979**, 100–101.

(61) (a) Dolak, T. M.; Bryson, T. A. *Tetrahedron Lett.* **1977**, 1961–64. (b) Cohen, T.; Abraham, W. D.; Myers, M. *J. Am. Chem. Soc.* **1987**, *109*, 7923–7924.

(62) Strzalko, T.; Seyden-Penne, J.; Wartski, L.; Corset, J.; Castellavventura, M.; Froment, F. *J. Org. Chem.* **1998**, *63*, 3295–3301.

(63) (a) Hüning, S.; Wehner, G. *Chem. Ber.* **1980**, *113*, 302–323. (b) Hüning, S.; Wehner, G. *Chem. Ber.* **1980**, *113*, 324–332.

(64) Sauvetre, R.; Roux-Schmitt, M.-C.; Seyden-Penne, J. *Tetrahedron* **1978**, *34*, 2135–2140.

(65) Reich, H. J.; Biddle, M. M.; Edmonston, R. J. *J. Org. Chem.* **2005**, *70*, 3375–3382.

(66) Arnett, E. M.; Moe, K. D. *J. Am. Chem. Soc.* **1991**, *113*, 7288–7293.

(67) Reich, H. J.; Sanders, A. W.; Fiedler, A. T.; Bevan, M. J. *J. Am. Chem. Soc.* **2002**, *124*, 13386–13387.

(68) Whisler, M. C.; MacNeil, S.; Snieckus, V.; Beak, P. *Angew. Chem., Int. Ed.* **2004**, *43*, 2206–2225.

(69) (a) McGarrity, J. F.; Ogle, C. A.; Brich, Z.; Loosli, H.-R. *J. Am. Chem. Soc.* **1985**, *107*, 1810–1815. (b) McGarrity, J. F.; Ogle, C. A. *J. Am. Chem. Soc.* **1985**, *107*, 1805–1810.

(70) This RINMR aldol study was done in hexane at  $-80\text{ }^{\circ}\text{C}$ : Palmer, C. A.; Ogle, C. A.; Arnett, E. M. *J. Am. Chem. Soc.* **1992**, *114*, 5619–5925.

(71) Dave Collum likes to quote an old aphorism: “if you find a lion that can talk, he will not tell you much about normal lions,” a problem which pervades mechanistic organolithium chemistry, including some of the results presented here. Collum, D. B.; McNeil, A. J.; Ramirez, A. *Angew. Chem., Int. Ed.* **2007**, *46*, 3002–3017.

(72) Al-Aseer, M. A.; Smith, S. G. *J. Org. Chem.* **1984**, *49*, 2608–2613. Al-Aseer, M. A.; Allison, B. D.; Smith, S. G. *J. Org. Chem.* **1985**, *50*, 2715–2719.

(73) Rogers, H. R.; Houk, J. *J. Am. Chem. Soc.* **1982**, *104*, 522.

(74) Bailey, W. F.; Luderer, M. R.; Jordan, K. P. *J. Org. Chem.* **2006**, *71*, 2825–2828.

(75) (a) West, P.; Waack, R.; Purmort, J. I. *J. Am. Chem. Soc.* **1970**, *92*, 840–845. (b) Waack, R.; Doran, M. A. *J. Am. Chem. Soc.* **1969**, *91*, 2456–2461.

(76) Bartlett, P. D.; Goebel, C. V.; Weber, W. P. *J. Am. Chem. Soc.* **1969**, *91*, 7425–7434.

(77) Sikorski, W. H.; Sanders, A. W.; Reich, H. J. *Magn. Reson. Chem.* **1998**, *36*, S118–S124.

(78) (a) WINDNMR. Reich, H. J. *J. Chem. Educ. Software* **1996**, *3D*, 2; <http://www.chem.wisc.edu/areas/reich/plt/windnmr.htm>. (b) WINPLT. <http://www.chem.wisc.edu/areas/reich/plt/winplt.htm>.

(79) (a) Bordwell DMSO pKa table: <http://www.chem.wisc.edu/areas/reich/pkatable/index.htm>. (b) Total syntheses of natural products: <http://www.chem.wisc.edu/areas/reich/syntheses/syntheses.htm>.